

1   **An antisense RNA capable of modulating the  
2   expression of the tumor suppressor microRNA-34a**  
3

4   **Jason T. Serviss<sup>1\*</sup>, Felix Clemens Richter, Nathanael Johansson  
5   Andrews<sup>1</sup>, Miranda Houtman, Laura Schwarzmüller, Per Johnsson,  
6   Jimmy Van Den Eynden, Erik Larsson<sup>2</sup>, Dan Grandér<sup>1</sup>, Katja Pokrovskaia  
7   Tamm<sup>1</sup>**

8  
9   <sup>1</sup> Department of Oncology and Pathology, Karolinska Institutet, Stockholm,  
10   Sweden

11   <sup>2</sup>Department of Medical Biochemistry and Cell Biology, Institute of  
12   Biomedicine, The Sahlgrenska Academy, University of Gothenburg, SE-405  
13   30 Gothenburg, Sweden

14   **\* Correspondence:**

15   Jason T. Serviss, Department of Oncology and Pathology, Karolinska  
16   Institutet, Stockholm, Sweden, SE-17177. [jason.serviss@ki.se](mailto:jason.serviss@ki.se)

17   **Abstract**

18   Long non-coding RNAs transcribed in an antisense orientation to sense  
19   protein-coding genes have been increasingly shown to play pivotal roles in  
20   regulating gene expression in both *cis* and *trans*. Expression of these  
21   antisense transcripts has often been shown to be dys-regulated in cancer  
22   giving rise to an altered expression of the corresponding sense gene. Here we  
23   describe the ability of a human antisense RNA to regulate levels of  
24   the *miR34a* tumor suppressor gene. *miR34a* is a downstream target  
25   of *TP53* and mediates critical cellular functions such as cellular growth and  
26   senescence. We find that the *miR34a* antisense RNA, a long non-coding RNA  
27   transcribed antisense to *miR34a*, is critical for *miR34a* expression and  
28   mediation of its cellular functions.

29  
30   **Introduction**

36 In recent years advances in functional genomics has revolutionized our  
37 understanding of the human genome. Evidence now points to the fact that  
38 approximately 75% of the genome is transcribed but only ~1.2% of this is  
39 responsible for encoding proteins (International Human Genome Sequencing  
40 2004, Djebali et al. 2012). The newly discovered non-coding elements have  
41 been categorized dependent on their function, size, localization, and  
42 orientation although a strict definition of these categories is an ongoing  
43 process. Of these recently identified elements, long non-coding (lnc) RNAs  
44 are defined as transcripts exceeding 200bp in length with a lack of a  
45 functional open reading frame. lncRNAs tend to exhibit increased tissue  
46 specificity, decreased expression levels, and less conservation than protein  
47 coding genes (Derrien et al. 2012). The vast prevalence of transcribed  
48 lncRNAs throughout the genome originally led to the speculation that these  
49 transcripts were non-functional “transcriptional relics” although further  
50 investigation has found lncRNAs to have important regulatory functions in  
51 processes such as development, cell fate, and oncogenesis (Rinn et al. 2007,  
52 Struhl 2007, Yap et al. 2010). Although many lncRNAs have been identified,  
53 the majority still have an unknown biological role and are yet to be functionally  
54 characterized (Derrien et al. 2012).

55

56 Some lncRNAs are dually classified as antisense (as) RNAs that are  
57 expressed from the same locus as a sense transcript in an antisense  
58 orientation. The phenomenon of asRNA transcription has been described in a  
59 large variety of eukaryotic organisms and was first discovered long before the  
60 advent of modern sequencing technologies (Wagner et al. 1994, Vanhee-

61 Brossollet et al. 1998). With new high-throughput transcriptome sequencing,  
62 current estimates indicate that up to 20-40% of the estimated 20,000 protein-  
63 coding genes exhibit antisense transcription (Chen et al. 2004, Katayama et  
64 al. 2005, Ozsolak et al. 2010). asRNAs have been shown to be expressed in  
65 both a concordant and discordant fashion with their sense transcript and can  
66 arise from independent promoters, bi-directional promoters exhibiting  
67 divergent transcription, as well as cryptic promoters (Core et al. 2008, Seila et  
68 al. 2008, Neil et al. 2009, Sigova et al. 2013). Examples of asRNA-mediated  
69 gene regulation are becoming increasingly prevalent and are often, but not  
70 exclusively, mediated in *cis* resulting in the modulation of sense gene levels.  
71 The mechanisms by which they accomplish this are largely diverse stretching  
72 from recruitment of chromatin modifying factors (Rinn et al. 2007), acting as  
73 microRNA (miRNA) sponges (Memczak et al. 2013), and causing  
74 transcriptional interference (Conley et al. 2012).

75

76 The hypothesis that asRNAs play an important role in oncogenesis was first  
77 proposed when studies increasingly found examples of aberrant expression of  
78 these transcripts and other lncRNA subgroups in tumor samples (Balbin et al.  
79 2015). Functional characterization of individual transcripts led to the discovery  
80 of asRNA-mediated regulation of several known tumorigenic factors. For  
81 example, the asRNA ANRIL was found to be up-regulated in leukemia and to  
82 function by repressing CDKN2B, an important regulator of cell cycle G1  
83 progression (Yap et al. 2010). Furthermore, the tumor suppressor PTEN has  
84 been shown to be regulated both transcriptionally and post-transcriptionally by  
85 asRNA transcripts (Johnsson et al. 2013). In addition, the

86 asRNA *HOTAIR* has been shown to negatively regulate the *HOXD* locus via  
87 recruitment of Polycomb Repressive Complex 2 mediating epigenetic  
88 silencing (Rinn et al. 2007). Although studies characterizing the functional  
89 importance of asRNAs in cancer are limited to date, it is becoming  
90 increasingly apparent that they play critical roles in regulating key cancer  
91 initiation and progression pathways; reviewed in (Spizzo et al. 2012).

92

93 Responses to cellular stress, e.g. DNA damage, sustained oncogene  
94 expression, and nutrient deprivation, are all tightly monitored and orchestrated  
95 cellular pathways that are commonly dys-regulated in cancer. Cellular  
96 signaling in response to these types of cellular stress often converge on the  
97 transcription factor *TP53* that regulates transcription of coding and non-coding  
98 downstream targets. One non-coding target of *TP53* is the tumor suppressor  
99 microRNA known as *miR34a* (Raver-Shapira et al. 2007).  
100 Upon *TP53* activation *miR34a* expression is increased allowing it to down-  
101 regulate its targets involved in cellular pathways such as, growth factor  
102 signaling, apoptosis, differentiation, and cellular senescence (Lal et al. 2011,  
103 Slabakova et al. 2017). *miR34a* is a crucial factor in mediating activated *TP53*  
104 response and it is often deleted or down-regulated in human cancers and has  
105 also been shown to be a valuable prognostic marker (Cole et al. 2008,  
106 Gallardo et al. 2009, Zenz et al. 2009, Cheng et al. 2010, Liu et al. 2011).  
107 Reduced *miR34a* transcription has been shown to be mediated via epigenetic  
108 regulation in many solid tumors, such as colorectal-, pancreatic-, and ovarian  
109 cancer (Vogt et al. 2011), as well as multiple types of hematological  
110 malignancies (Chim et al. 2010). In addition, *miR34a* has been shown to be

111 transcriptionally regulated via TP53 homologs, TP63 and TP73, other  
112 transcription factors, e.g. STAT3 and MYC, and, in addition, post-  
113 transcriptionally through miRNA sponging by the NEAT1 lncRNA (Chang et al.  
114 2008, Su et al. 2010, Agostini et al. 2011, Rokavec et al. 2015, Ding et al.  
115 2017). Despite these findings, the mechanisms underlying miR34a regulation  
116 in the context of oncogenesis have not yet been fully elucidated.

117

118 Multiple studies across different cancers have reported a decrease in  
119 oncogenic phenotypes when miR34a expression is induced in a p53-null  
120 background, although endogenous mechanisms for achieving this have not  
121 yet been discovered (Liu et al. 2011, Ahn et al. 2012, Yang et al. 2012,  
122 Stahlhut et al. 2015, Wang et al. 2015). In addition, previous reports have  
123 identified a lncRNA originating in the antisense orientation from the miR34a  
124 locus which is regulated by TP53 and is induced upon cellular stress (Rashi-  
125 Elkeles et al. 2014, Hunten et al. 2015, Leveille et al. 2015, Ashouri et al.  
126 2016, Kim et al. 2017). Despite this, none of these studies have continued to  
127 functionally characterize this transcript. In this study we functionally  
128 characterize the *miR34a* asRNA transcript, finding that modulating the levels  
129 of the *miR34a* asRNA is sufficient to increase levels of *miR34a* and results in  
130 a decrease of multiple tumorigenic phenotypes. Furthermore, we find that  
131 miR34a asRNA-mediated up-regulation of miR34a is sufficient to induce  
132 endogenous cellular mechanisms counteracting several types of stress stimuli  
133 in a TP53 deficient background.

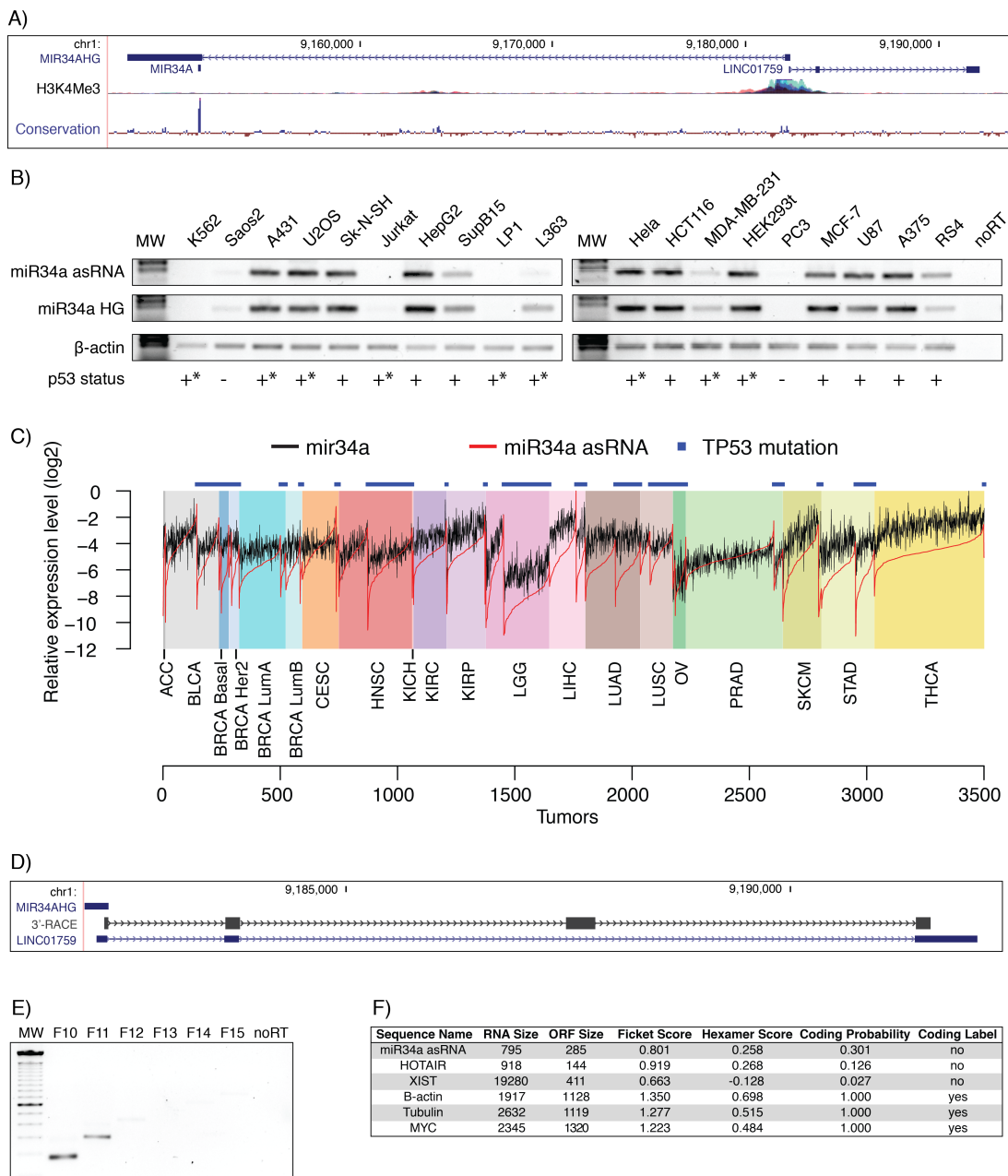
134

135 **Results**

136

137     **Characterization of the *miR34a* asRNA transcript**

138  
139     In order to evaluate possible asRNA-mediated regulation of *miR34a*  
140     expression, we began by examining evidence for asRNA transcripts at the  
141     *miR34a* locus. This revealed an annotated lncRNA (*LINC01759*, also known  
142     as *RP3-510D11.2*) transcript in a “head-to-head” orientation with  
143     approximately 100 base pair overlap with the *miR34a* HG, hereafter referred  
144     to as *miR34a* asRNA (**Fig. 1a**). Sentence about conservation and H3K4 at  
145     locus? Due to the fact that sense/antisense pairs can be either concordantly  
146     or discordantly expressed we next sought to evaluate this relationship in the  
147     case of *miR34a* HG and asRNA. Using a diverse panel of cancer cell lines,  
148     we were able to detect co-expression of both the *miR34a* HG  
149     and *miR34a* asRNA (**Fig. 1b**). We included *TP53*+/+, *TP53*  
150     mutated, and *TP53*-/ cell lines in the panel due to previous reports  
151     that *miR34a* is a known downstream target of *TP53*. These results indicate  
152     that *miR34a* HG and *miR34a* asRNA are co-expressed and that their  
153     expression levels correlate with *TP53* status, with *TP53*+/+ cell lines tending  
154     to have higher expression of both transcripts.



155

156 **Figure 1: Characterization of the *miR34a* asRNA transcript.** A) A schematic picture of  
 157 the *miR34a* locus from UCSC genome browser (hg38) including *miR34a* HG and mature *miR34a*, and  
 158 *LINC01759*. H3K4me3 ChIP-seq data and conservation over the locus is also shown. B) Semi-  
 159 quantitative PCR data from the screening of a panel of cancer cell lines. \* Indicates wild-  
 160 type *TP53* with mechanisms present, which inhibit *TP53* function (such as SV40 large T antigen in the  
 161 case of HEK293T cells). C) A graphical depiction of the TCGA correlation analysis. The *TP53* mutated  
 162 samples only include non-synonymous *TP53* mutations. Adrenocortical carcinoma (ACC), Bladder  
 163 Urothelial Carcinoma (BLCA), Breast invasive carcinoma (BRCA), Head and Neck squamous cell  
 164 carcinoma (HNSC), Kidney Chromophobe (KICH), Lower Grade Glioma (LGG), Liver hepatocellular  
 165 carcinoma (LIHC), Ovarian serous cystadenocarcinoma (OV), Prostate adenocarcinoma (PRAD), Skin  
 166 Cutaneous Melanoma (SKCM), Stomach adenocarcinoma (STAD). D) 3'-RACE sequencing results  
 167 together with the annotated *miR34a* asRNA (*LINC01759*). E) Semi-quantitative PCR results from the  
 168 primer walk assay performed using HEK293T cells. F) Coding potential analysis assessed using the  
 169 Coding-potential Assessment Tool including *miR34a* asRNA and two characterized lncRNA transcripts  
 170 (*HOTAIR* and *XIST*) and three known protein coding transcripts (*β-actin*, *tubulin*, and *MYC*).  
 171

172 We next sought to interrogate primary cancer samples to examine if a  
173 correlation between *miR34a* asRNA and *miR34a* expression levels could be  
174 identified. For this task we utilized RNA sequencing data from The Cancer  
175 Genome Atlas (TCGA) after stratifying patients by cancer type, *TP53* status  
176 and, in select cases, cancer subtypes. The results indicate  
177 that *miR34a* asRNA and *miR34a* expression are strongly correlated in the  
178 vast majority of cancer types examined, both in the presence and absence of  
179 wild-type *TP53* (**Fig. 1c, Supplementary Fig. 1a**). The results also further  
180 confirm that the expression of both *miR34a* and its asRNA have a tendency to  
181 be reduced in patients with non-synonymous *TP53* mutations.

182

183 Next, we aimed to gain a thorough understanding of *miR34a* asRNA's  
184 molecular characteristics and cellular localization. Polyadenylation status was  
185 evaluated via cDNA synthesis with either random nanomers or oligoDT  
186 primers followed by semi-quantitative PCR with results indicating that  
187 the *miR34a* asRNA is polyadenylated although the unspliced form seems to  
188 only be in the polyA negative state (**Supplementary Fig. 1c**). To  
189 experimentally determine the 3' termination site for the *miR34a* asRNA  
190 transcript we performed 3' rapid amplification of cDNA ends (RACE) using the  
191 U2OS osteosarcoma cell line that exhibited high endogenous levels  
192 of *miR34a* asRNA in the cell panel screening. Sequencing of the resulting  
193 cloned cDNA indicated the transcripts 3' transcription termination site to be  
194 525 base pairs upstream of the *LINC01759* transcript's annotated termination  
195 site (**Fig. 1d**). Next, we characterized the *miR34a* asRNA 5' transcription start  
196 site by carrying out a primer walk assay. A common reverse primer was

197 placed in exon 2 and forward primers were gradually staggered upstream of  
198 the transcripts annotated start site (**Supplementary Fig. 1b**). Our results  
199 indicated that the 5' start site for *miR34a* asRNA is in fact approximately 90bp  
200 (F11 primer) to 220bp (F12 primer) upstream of the annotated start site (**Fig.**  
201 **1e**). We furthermore investigated the propensity of *miR34a* asRNA to be  
202 alternatively spliced, using PCR cloning and sequencing and found that the  
203 transcript is post-transcriptionally spliced to form multiple different isoforms  
204 (**Supplementary Fig. 1d**). \*make an additional supplementary figure showing  
205 spliced RNAseq reads\* Finally, to evaluate the cellular localization of miR34a  
206 asRNA we utilized RNA sequencing data from five cancer cell lines included  
207 in the ENCODE (Consortium 2012) project that had been fractionated into  
208 cytosolic and nuclear fractions. The analysis revealed that the *miR34a* asRNA  
209 transcript localizes to both the nucleus and cytoplasm but primarily resides in  
210 the nucleus (**Supplementary Fig. 1f**).

211

212 Finally, we utilized multiple approaches to evaluate the coding potential of  
213 the *miR34a* asRNA transcript. The Coding-Potential Assessment Tool is a  
214 bioinformatics-based tool that uses a logistic regression model to evaluate  
215 coding-potential by examining ORF length, ORF coverage, Fickett score and  
216 hexamer score (Wang et al. 2013). Results indicated that *miR34a* asRNA has  
217 a similar lack of coding capacity to the known non-coding  
218 transcripts *HOTAIR* and *XIST* and differs greatly when examining these  
219 parameters to the known coding transcripts  $\beta$ -actin, tubulin, and *MYC* (**Fig.**  
220 **1F**). We further confirmed these results using the Coding-Potential Calculator  
221 that utilizes a support based machine-based classifier and accesses an

222 alternate set of discriminatory features (**Supplementary Fig. 1E**) (Kong et al.  
223 2007). \*To fully evaluate coding potential methods such as mass  
224 spectrometry or ribosome profiling must be used, however *miR34a* asRNA  
225 presents little evidence of coding potential as evaluated by these two  
226 bioinformatic approaches (31) [31]. We hope to be able to scan for peptides  
227 matching to *miR34a* asRNA in TCGA before submission and, instead, will  
228 mention results here....\*

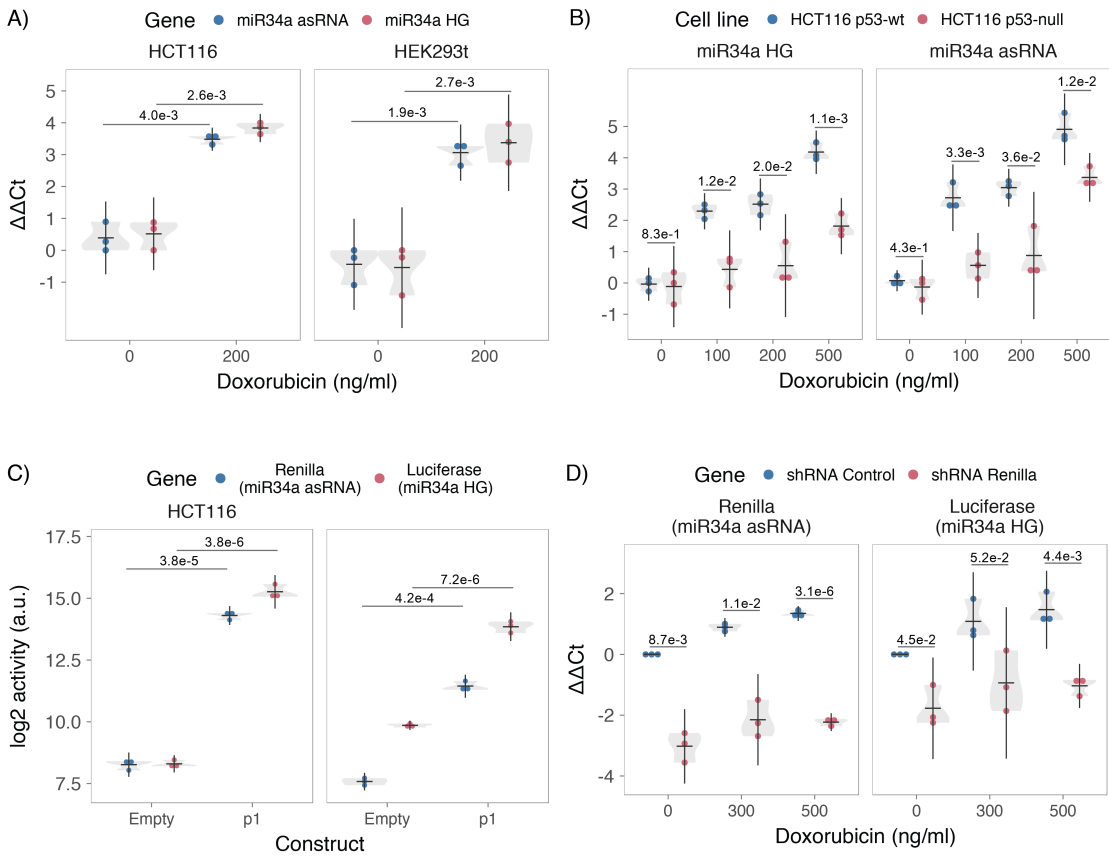
229

230 ***TP53-mediated regulation of miR34a asRNA expression***

231 *miR34a* is a known downstream target of TP53 and has been previously  
232 shown to exhibit increased expression within multiple contexts of cellular  
233 stress. Due to the strong correlation between *miR34a* and *miR34a* asRNA  
234 expression, we hypothesized that *miR34a* asRNA may be regulated in a  
235 similar fashion whereby transcription is stimulated by the activation of TP53.  
236 To test this, we treated HEK293t, embryonic kidney cells, and HCT116,  
237 colorectal cancer cells, with the DNA damaging agent doxorubicin to activate  
238 TP53. QPCR-mediated measurement of both *miR34a* HG and asRNA  
239 indicated that their expression levels were increased in response to  
240 doxorubicin treatment in both cell lines (**Fig. 2a**). This result corresponds well  
241 with previous reports of *miR34a* asRNA response in other biological contexts  
242 (Rashi-Elkeles et al. 2014, Hunten et al. 2015, Leveille et al. 2015, Ashouri et  
243 al. 2016, Kim et al. 2017). To access if it is in fact *TP53* that is responsible for  
244 the increase in *miR34a* asRNA expression upon DNA damage, we  
245 treated *TP53*<sup>+/+</sup> and *TP53*<sup>-/-</sup> HCT116 cells with increasing concentrations of the  
246 doxorubicin and monitored the expression of both *miR34a* HG and asRNA.

247 We observed a dose-dependent increase in both *miR34a* HG and asRNA  
248 expression levels with increasing amounts of doxorubicin, indicating that  
249 these two transcripts are co-regulated, although, this effect was largely  
250 abrogated in *TP53*<sup>-/-</sup> cells (**Fig. 2b**). These results indicate  
251 that *TP53* activation increases *miR34a* asRNA expression upon the induction  
252 of DNA damage. Despite this, *TP53*<sup>-/-</sup> cells also showed a dose dependent  
253 increase in both *miR34a* HG and asRNA, indicating that additional factors,  
254 other than *TP53*, are capable of initiating an increase in expression of both of  
255 these transcripts upon DNA damage.

256



257

258 **Figure 2: TP53-mediated regulation of the *miR34a* locus.** A) Evaluating the effects of 24 hours of  
259 treatment with 200 ng/ml doxorubicin on *miR34a*asRNA and HG in HCT116 and HEK293t  
260 cells.\* B) Monitoring *miR34a* HG and asRNA expression levels during 24 hours doxorubicin treatment  
261 in *TP53*<sup>+/+</sup> and *TP53*<sup>-/-</sup> HCT116 cells.\* C) Quantification of luciferase and renilla levels after  
262 transfection of HCT116 and HEK293T cells with the p1 construct.\* D) HCT116 cells were co-  
263 transfected with the p1 construct and shRNA renilla or shRNA control and subsequently treated with  
264 increasing doses of doxorubicin. 24 hours post-treatment, cells were harvested and renilla and  
265 luciferase levels were measured using QPCR. Resulting p-values from statistical testing are shown  
266 above the shRenilla samples which were compared to the shRNA control using the respective treatment  
267 condition.\* \*Individual points represent results from independent experiments and the gray shadow  
268 indicates the density of those points. Error bars show the 95% CI, black horizontal lines represent the  
269 mean, and p-values are shown over long horizontal lines indicating the comparison tested.  
270

271 It is likely, due to the head-to head orientation of *miR34a* HG and asRNA, that  
272 transcription may be initiated from a single promoter in a bi-directional  
273 manner. To investigate whether *miR34a* HG and asRNA are transcribed from  
274 the same promoter as divergent transcripts, we cloned the *miR34a* HG  
275 promoter, including the *TP53* binding site, into a luciferase/renilla dual  
276 reporter vector which we hereafter refer to as p1 (**Supplementary Fig. 2a**  
277 **and 2b**). Upon transfection of p1 into HCT116 and HEK293t cell lines we  
278 observed increases in both luciferase and renilla indicating that *miR34a* HG  
279 and asRNA expression can be regulated by a single promoter contained  
280 within the p1 construct (**Fig. 2c**).

281

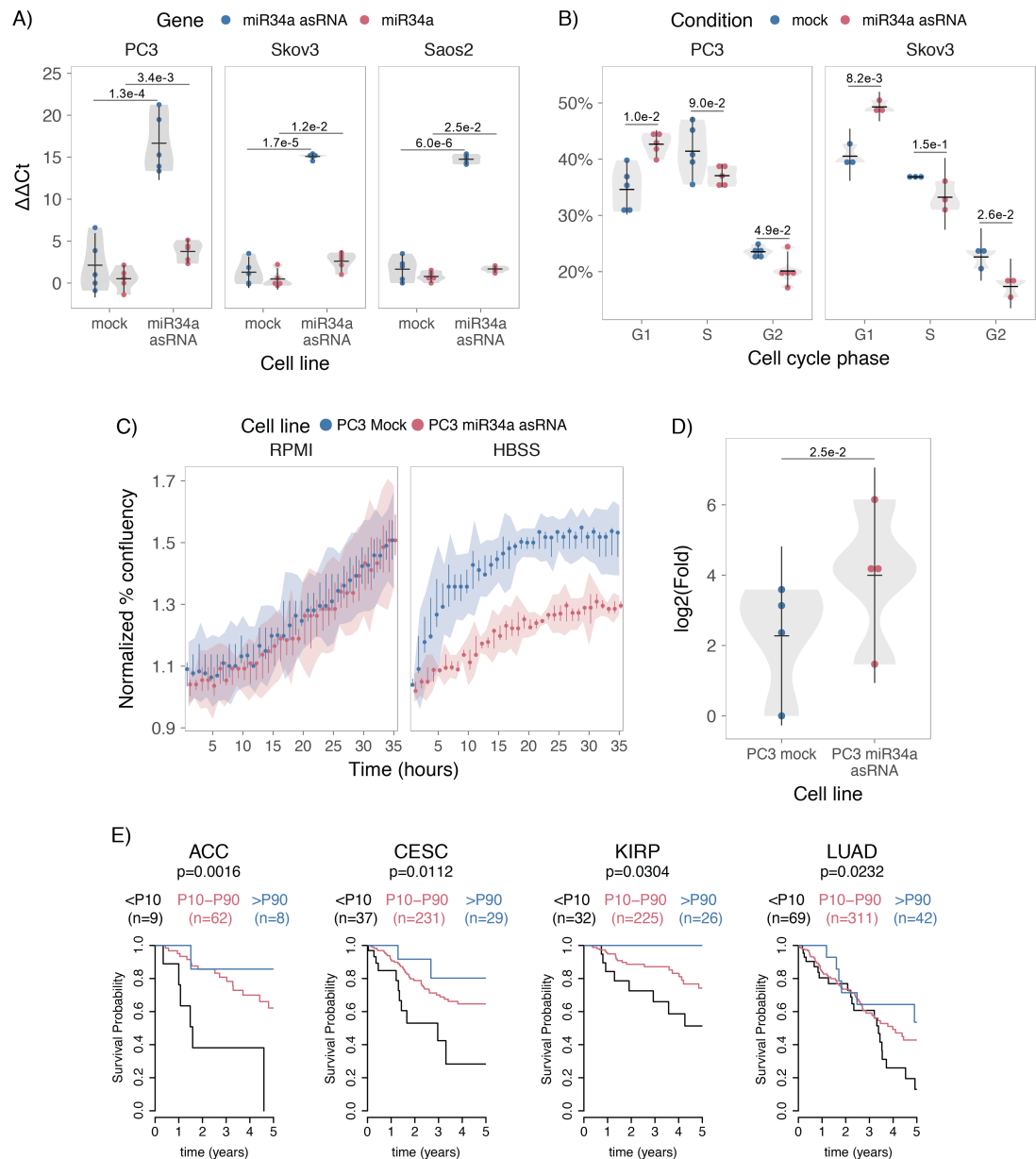
282 Functional characterization of individual antisense transcripts has previously  
283 shown their capability to regulate their sense gene (Yap et al. 2010,  
284 Pelechano et al. 2013). We therefore investigated the possibility  
285 that *miR34a* asRNA may regulate *miR34a* HG levels. We hypothesized that  
286 the overlapping regions of the sense and antisense transcripts may have a  
287 crucial role in *miR34a* asRNAs ability to regulate *miR34a* HG, possibly via  
288 RNA:DNA or RNA:RNA interaction. Accordingly, we first co-transfected the p1  
289 construct, containing the overlapping region of the two transcripts, and a short  
290 hairpin (sh) RNA targeting renilla into HCT116 cells subsequently treating  
291 them with increasing doses doxorubicin. Analysis of luciferase and renilla  
292 expression revealed that shRNA-mediated knock down of the renilla transcript  
293 (corresponding to *miR34a* asRNA) caused luciferase (corresponding  
294 to *miR34a* HG) levels to concomitantly decrease (**Fig. 2d**). Collectively, these  
295 results indicate that *miR34a* asRNA positively regulates levels of *miR34a* HG

296 and is crucial for an appropriate TP53-mediated *miR34a* response to DNA  
297 damage.

298

299 **Functional analysis of *miR34a* asRNA in *TP53*-deficient cells**

300 Despite the fact that *TP53* regulates *miR34a* HG and asRNA expression, our  
301 results indicated that other factors are also able to regulate this locus (**Fig.**  
302 **2b**). Utilizing a lentiviral system, we stably over-expressed the *miR34a* asRNA  
303 transcript in three *TP53*-null cell lines; PC3 (prostate cancer), Saos2  
304 (osteogenic sarcoma), and Skov3 (adenocarcinoma). We first analyzed the  
305 levels of *miR34a* asRNA in these stable over-expression cell lines, compared  
306 to HEK293T cells, which have high endogenous levels of *miR34a* asRNA,  
307 finding that, on average, the over-expression was approximately 30-fold  
308 higher in the over-expression cell lines than in HEK293t cells. Due to the fact  
309 that *miR34a* asRNA can be up-regulated ~30-fold in response to DNA  
310 damage (**Fig. 2b**), we deemed this over-expression level to correspond to  
311 physiologically relevant levels in cells encountering a stress stimulus, such as  
312 DNA damage (**Supplementary Fig. 3a**). Analysis of *miR34a* levels in  
313 the *miR34a* asRNA over-expressing cell lines showed that *miR34a* asRNA  
314 over-expression resulted in a concomitant increase in the expression  
315 of *miR34a* in all three cell lines (**Fig. 3a**). These results indicate that, in the  
316 absence of TP53, *miR34a* expression may be rescued by increasing the  
317 levels of *miR34a* asRNA expression.



318

319 **Figure 3: miR34a asRNA positively regulates miR34a and its associated phenotypes.** A) QPCR-  
320 mediated quantification of miR34a expression in cell lines stably over-  
321 expressing miR34a asRNA.\* B) Cell cycle analysis comparing stably over-expressing miR34a asRNA  
322 cells to the respective mock expressing cells.\* C) Analysis of cellular growth over time in miR34a  
323 asRNA over-expressing PC3 cells. Points represent the median from 3 independent experiments and  
324 the colored shadows indicate the 95% confidence interval. D) Differential phosphorylated polymerase  
325 II binding in miR34a asRNA over-expressing PC3 cells.\* E) Survival analysis dependent  
326 on miR34a asRNA expression levels using TCGA data. P10 = 10%, P10-P90 = 10%-90%, P90 = 90%.  
327 Adrenocortical carcinoma (ACC), Cervical squamous cell carcinoma and endocervical adenocarcinoma  
328 (CESC), Kidney renal papillary cell carcinoma (KIRP), Lung adenocarcinoma (LUAD). \*Individual  
329 points represent results from independent experiments and the gray shadow indicates the density of  
330 those points. Error bars show the 95% CI, black horizontal lines represent the mean, and p-values are  
331 shown over long horizontal lines indicating the comparison tested.  
332

333 *miR34a* has been previously shown to regulate cell cycle progression, with  
334 increasing levels of *miR34a* causing senescence via G1 arrest. Cell cycle  
335 analysis via determination of DNA content showed a significant increase in G1  
336 phase cells in the PC3 and Skov3 *miR34a* asRNA over-expressing cell lines,  
337 indicative of G1 arrest, as well as, a significant decrease of cells in G2 phase  
338 (**Fig. 3b**). *miR34a*'s effects on the cell cycle are mediated by its ability to  
339 target cell cycle regulators such as cyclin D1 (*CCND1*) (Sun et al. 2008). We  
340 therefore sought to determine if the *miR34a* asRNA over-expressing cell lines  
341 exhibited effects on these known *miR34a* targets. Quantification of  
342 both *CCND1* RNA expression (**Supplementary Fig. 3b**) and protein levels  
343 (**Supplementary Fig. 3c**) in the PC3 *miR34a* asRNA over-expressing cell line  
344 showed a significant decrease of *CCND1* levels in *miR34a* asRNA over-  
345 expressing cell lines compared to the mock control.

346  
347 *miR34a* is also a well known inhibitor of cellular growth via its ability to  
348 regulate growth factor signaling. Furthermore, starvation has been shown to  
349 induce *miR34a* expression that down-regulates multiple targets that aid in the  
350 phosphorylation of multiple pro-survival and growth factors (Lal et al. 2011).  
351 We further interrogated the effects of *miR34a* asRNA over-expression by  
352 investigating the growth rate of the cells in both normal and starvation  
353 conditions by measuring confluence over a 35-hour period. Although under  
354 normal growth conditions there is only a marginal trend towards decreased  
355 growth at individual early time points in *miR34a* asRNA over-expressing cell  
356 lines, these effects on cell growth are drastically increased in starvation  
357 conditions. This is in accordance with our previous results, indicating

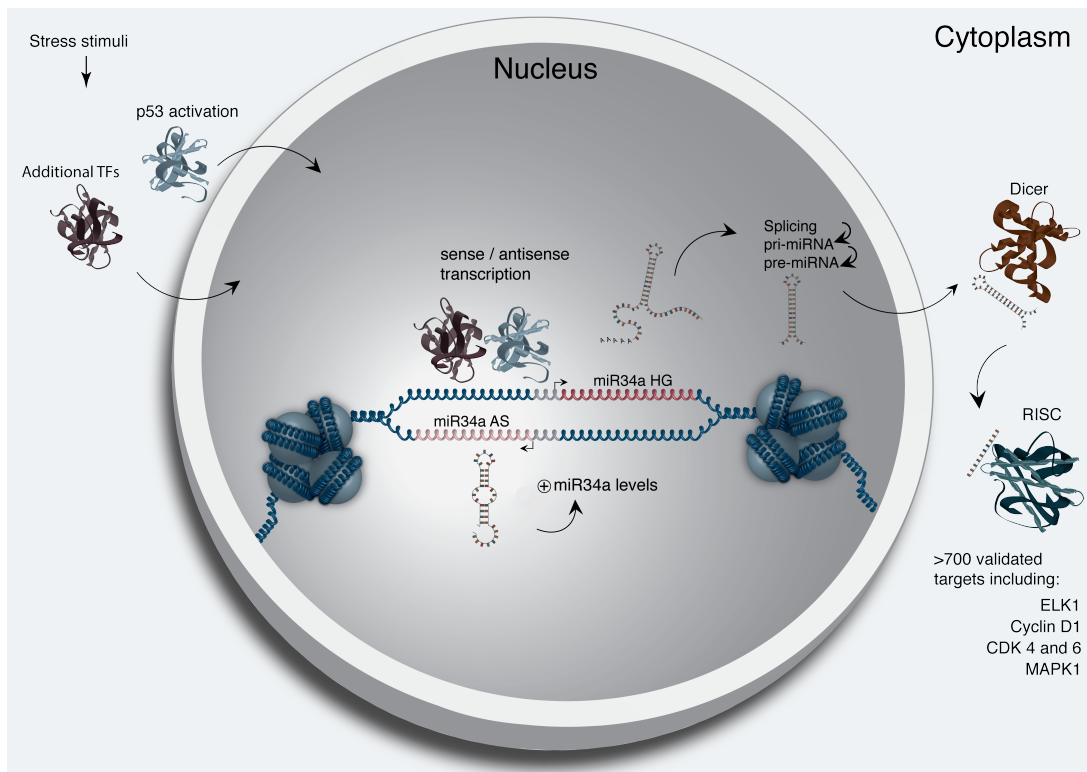
358 that, *miR34a* asRNA-mediated increases in *miR34a* expression are especially  
359 crucial under conditions of stress and necessary for the initiation of an  
360 appropriate cellular response. In summary, we find that over-expression  
361 of *miR34a* asRNA is sufficient to increase *miR34a* expression and gives rise  
362 to known phenotypes observed with increased *miR34a* expression.

363

364 Antisense RNAs have been reported to mediate their effects both via  
365 transcriptional and post-transcriptional mechanisms. Due to the fact that  
366 *miR34a* expression is undetected in wild type PC3 cells but, upon over-  
367 expression of *miR34a* asRNA, increases to detectable levels, we  
368 hypothesized that *miR34a* asRNA is capable of regulating *miR34a* expression  
369 levels via transcriptional mechanisms. To ascertain if this is actually the case,  
370 we performed chromatin immunoprecipitation (ChIP) for phosphorylated  
371 polymerase II (polII) at the *miR34a* HG promoter in both *miR34a* asRNA over-  
372 expressing and mock control cell lines. Our results indicated a clear increase  
373 in phosphorylated polII binding at the *miR34a* promoter upon *miR34a* asRNA  
374 over-expression indicating *miR34a* asRNA's ability to regulate *miR34a* levels  
375 on a transcriptional level (**Fig. 3d**).

376

377 \*Finally, we investigated if *miR34a* asRNA levels affected the survival of  
378 patients across a broad range of cancer types within the TCGA study. Of the  
379 cancer types examined, we identified four where increased *miR34a* asRNA  
380 levels gave rise to a beneficial prognosis (**Fig 3g**). This figure will either be  
381 removed or modified before submission\*



382

383 **Figure 4: A graphical summary of the proposed *miR34a* asRNA function.** Stress stimuli,  
384 originating in the cytoplasm or nucleus, activates *TP53* as well as additional factors. These factors then  
385 bind to the *miR34a* promoter and drive transcription of the sense and antisense strands. *miR34a* asRNA  
386 serves to increase the levels of *miR34a* HG transcription via an unknown mechanism. *miR34a* HG  
387 then, in turn, is then spliced, processed by the RNase III enzyme Drosha, and exported to the  
388 cytoplasm. The *miR34a* pre-miRNA then binds to Dicer where the hair-pin loop is cleaved and  
389 mature *miR34a* is formed. Binding of the mature *miR34a* miRNA to the RISC complex then allows it  
390 to bind and repress its targets.  
391

392 **Discussion**

393  
394 Multiple studies have previously shown asRNAs to be crucial for the  
395 appropriate regulation of cancer-associated protein-coding genes and that  
396 their dys-regulation can lead to perturbation of tumor suppressive and  
397 oncogenic pathways, as well as, cancer-related phenotypes. Here we show  
398 that asRNAs are also capable of regulating cancer-associated miRNAs  
399 resulting in similar consequences as protein-coding gene dys-regulation (**Fig.**  
400 **4**). Interestingly, we show that, both in the presence and absence of  
401 *TP53*, *miR34a* asRNA provides an additional regulatory level and functions by  
402 mediating the increase of *miR34a* expression in both homeostasis and upon  
403 encountering multiple forms of cellular stress. Furthermore, we find that  
404 *miR34a* asRNA-mediated increases in *miR34a* expression levels are sufficient  
405 to drive the appropriate cellular responses to the forms of stress stimuli that  
406 are encountered. These results are also supported by others who have  
407 utilized various molecular biology methods to up regulate *miR34a* expression  
408 in a *p53* deficient background (Liu et al. 2011, Ahn et al. 2012, Yang et al.  
409 2012, Stahlhut et al. 2015, Wang et al. 2015).

410

411 In agreement with previous studies, we demonstrate that upon encountering  
412 various types of cellular stress, *TP53* in concert with additional factors bind  
413 and initiate transcription at the *miR34a* locus, thus increasing the levels of  
414 *miR34a* and, in addition, *miR34a* asRNA. We hypothesize that *miR34a*  
415 asRNA may form a positive feedback for *miR34a* expression whereby *miR34a*  
416 asRNA serves as a scaffold for the recruitment of additional factors that  
417 support the expression of *miR34a* and, thus, driving the cell towards a

418 reduction in growth factor signaling, senescence, and eventually apoptosis.  
419 On the other hand, in cells without a functional p53, other factors, which  
420 typically act independently or in concert with *TP53*, may initiate transcription  
421 of the *miR34a* locus. We believe that *miR34a* asRNA could potentially be  
422 interacting directly with one of these additional factors and recruiting it to the  
423 *miR34a* locus in order to drive *miR34a* transcription. This is especially  
424 plausible due to the fact that, due to the head-to-head orientation of the  
425 *miR34a* HG and asRNA, there is sequence complementarity between the  
426 RNA and the promoter DNA, although further work will need to be performed  
427 to ascertain if this binding actually takes place. \*\*\*add additional eClip data to  
428 supplementary and mention here? Incomplete figure attached to mail\*\*\*  
429

430 Despite the fact that the exact mechanism by which the *miR34a* asRNA  
431 operates is not elucidated in this study, several pieces of experimental  
432 evidence can provide insights concerning this. In both gain- and loss-of-  
433 function experiments (**Figure 2d, Figure 3a**) we note that it is the  
434 transcriptional product of the *miR34a* asRNA locus that gives rise to the effect  
435 on miR34a levels. This precludes the idea that transcription of *miR34a* asRNA  
436 may potentially be sufficient to increase the levels of *miR34a* and, instead,  
437 mechanisms must be in place which allow the direct or indirect interaction with  
438 the *miR34a* asRNA transcript to stimulate miR34a HG transcription.  
439 Furthermore, due to the fact that the p1 construct only contains a small  
440 portion of the *miR34a* asRNA transcript, it could be the case that this portion  
441 is sufficient to give rise to at least a partial *miR34a* inducing response (**Fig 2d,**  
442 **Supplementary Fig. 2a-2b**). Further studies may reveal that utilization of only

443 this short oligonucleotide may be sufficient to increase *miR34a* expression  
444 levels and thus provide a potential pathway towards oligonucleotide-mediated  
445 therapies. In fact, clinical trials utilizing *miR34a* replacement therapy have  
446 previously been conducted but, disappointingly, were terminated after adverse  
447 side effects of an immunological nature were observed in several of the  
448 patients. Although it is not presently clear if these side effects were caused by  
449 *miR34a* or the liposomal carrier used to deliver the miRNA, the multitude of  
450 evidence indicating *miR34a*'s crucial role in oncogenesis still makes its  
451 therapeutic induction a lucrative strategy for patient treatment and needs  
452 further investigation.

453

454 An unannotated transcript, *Lnc34a*, arising from the antisense orientation of  
455 the *miR34a* locus and with a transcription start site >250 bp upstream of the  
456 annotated *miR34a* asRNAs start site, has been previously reported in a study  
457 examining colorectal cancer (Wang et al. 2016). Among the findings in Wang  
458 et al. the authors discover that *Lnc34a* negatively regulates *miR34a*  
459 expression via recruitment of *DNMT3a*, *PHB2*, and *HDAC1* to the *miR34a*  
460 promoter. Although the *Lnc34a* and *miR34a* asRNA transcripts share some  
461 sequence similarity, we believe them to be separate RNAs that are,  
462 potentially, different isoforms of the same gene. Furthermore, we believe  
463 that *Lnc34a* may be highly context dependent and potentially only expressed  
464 at biologically significant levels in colon cancer stem cells, or other stem-like  
465 cells, in agreement with the conclusions drawn in the paper. We thoroughly  
466 address our reasons for these beliefs and give appropriate supporting  
467 evidence in (**Supplementary Results 4**). The fact that *Lnc34a* and *miR34a*

468 asRNA would appear to have opposing roles in their regulation of *miR34a*  
469 further underlines the complexity of the regulation at this locus.

470

471 In summary, our results indicate that *miR34a* asRNA is a vital player in the  
472 regulation of *miR34a* and is especially important in contexts where cellular  
473 stresses are encountered. Due to the fact that many of these stress stimuli  
474 are strongly associated with cancer, we believe *miR34a* asRNA's ability to  
475 fine-tune *miR34a* expression levels to be especially crucial in tumorigenesis.

476

## 477 **Materials and Methods**

### 478 **Cell culture**

479 All cell lines were cultured at 5% CO<sub>2</sub> and 37° C with HEK293T cells cultured  
480 in DMEM high glucose (Hyclone), HCT116 and U2OS cells in McCoy's 5a  
481 (Life Technologies), and PC3 cells in RPMI (Hyclone) and 2 mM L-glutamine  
482 **add other cell lines**. All growth mediums were supplemented with 10% heat-  
483 inactivated FBS and 50 µg/ml of streptomycin and 50 µg/ml of penicillin.

### 484 **Bioinformatics and Data availability**

486 The USCS genome browser (Kent et al. 2002) was utilized for the  
487 bioinformatic evaluation of antisense transcription utilizing the RefSeq  
488 (O'Leary et al. 2016) gene annotation track.

489 All raw experimental data, code used for analysis, and supplementary  
490 methods are available for review  
491 at [https://github.com/GranderLab/miR34a\\_asRNA\\_project](https://github.com/GranderLab/miR34a_asRNA_project) (Serviss 2017) and  
492 are provided as an R package. All analysis took place using the R statistical  
493 programming language (Team 2017) using multiple external packages that

494 are all documented in the package associated with the article (Wilkins , Chang  
495 2014, Wickham 2014, Wickham 2016, Allaire et al. 2017, Arnold 2017,  
496 Wickham 2017, Wickham 2017, Wickham 2017, Xiao 2017, Xie 2017). The  
497 package facilitates replication of the operating system and package versions  
498 used for the original analysis, reproduction of each individual figure included  
499 in the article, and easy review of the code used for all steps of the analysis,  
500 from raw-data to figure.

501

## 502 **Coding Potential**

503 Protein-coding capacity was evaluated using the Coding-potential  
504 Assessment Tool (Wang et al. 2013) and Coding-potential Calculator (Kong et  
505 al. 2007) with default settings. Transcript sequences for use with Coding-  
506 potential Assessment Tool were downloaded from the UCSC genome  
507 browser using the  
508 IDs: *HOTAIR* (ENST00000455246), *XIST* (ENST00000429829), β-actin  
509 (ENST00000331789), Tubulin (ENST00000427480),  
510 and *MYC* (ENST00000377970). Transcript sequences for use with Coding-  
511 potential Calculator were downloaded from the UCSC genome browser using  
512 the following IDs: *HOTAIR* (uc031qho.1), β-actin (uc003soq.4).

513

## 514 **shRNAs**

515 shRNA-expressing constructs were cloned into the U6M2 construct using the  
516 BgIII and KpnI restriction sites as previously described (Amarzguioui et al.  
517 2005) (Amarzguioui et al. 2005). shRNA constructs were transfected using  
518 Lipofectamine 2000 or 3000 (Life Technologies). The sequence targeting

519 renilla is as follows: AAT ACA CCG CGC TAC TGG C.

520

521 **Lentiviral particle production, infection, and selection.**

522 Lentivirus production was performed as previously described in (Turner et al.  
523 2012). Briefly, HEK293T cells were transfected with viral and expression  
524 constructs using Lipofectamine 2000 (Life Technologies), after which viral  
525 supernatants were harvested 48 and 72 hours post-transfection. Viral  
526 particles were concentrated using PEG-IT solution (Systems Biosciences)  
527 according to the manufacturer's recommendations. HEK293T cells were used  
528 for virus titration and GFP expression was evaluated 72hrs post-infection via  
529 flow cytometry after which TU/ml was calculated.

530

531 **Western Blotting.**

532 Samples were lysed in 50 mM Tris-HCl, pH 7.4, 1% NP-40, 150 mM NaCl, 1  
533 mM EDTA, 1% glycerol, 100 µM vanadate, protease inhibitor cocktail and  
534 PhosSTOP (Roche Diagnostics GmbH). Lysates were subjected to SDS-  
535 PAGE and transferred to PVDF membranes. The proteins were detected by  
536 western blot analysis by using an enhanced chemiluminescence system  
537 (Western Lightning-ECL, PerkinElmer). Antibodies used were specific  
538 for CCND1 (Cell Signaling, cat. no. 2926, 1:1000), and β-actin (Sigma-Aldrich,  
539 cat. no. A5441, 1:5000). All western blot quantifications were performed using  
540 ImageJ (Schneider et al. 2012).

541

542 **Generation of U6-expressed miR34a AS lentiviral constructs.**

543 The U6 promoter was amplified from the U6M2 cloning plasmid (Amarzguioui

544 et al. 2005) and ligated into the Not1 restriction site of the pHIV7-IMPDH2  
545 vector (Turner et al. 2012). miR43a asRNA was PCR amplified and  
546 subsequently cloned into the Nhe1 and Pac1 restriction sites in the pHIV7-  
547 IMPDH2-U6 plasmid.

548

549 **Promoter activity.**

550 Cells were co-transfected with the renilla/firefly bidirectional promoter  
551 construct (Polson et al. 2011) and GFP by using Lipofectamine 2000 (Life  
552 Technologies). The expression of GFP and luminescence was measured 24 h  
553 post transfection by using the Dual-Glo Luciferase Assay System (Promega)  
554 and detected by the GloMax-Multi+ Detection System (Promega). The  
555 expression of luminescence was normalized to GFP.

556

557 **Flow Cytometry.**

558 Cells were harvested, centrifuged and, either re-suspended in PBS, 5% FBS  
559 and analyzed for GFP expression using the LSRII machine (BD Biosciences).

560

561 **RNA extraction and cDNA synthesis.**

562 For downstream SYBR green applications, RNA was extracted using the  
563 RNeasy mini kit (Qiagen) and subsequently treated with DNase (Ambion  
564 Turbo DNA-free, Life Technologies). 500ng RNA was used for cDNA  
565 synthesis using MuMLV (Life Technologies) and a 1:1 mix of oligo(dT) and  
566 random nanomers.

567 For analysis of miRNA expression with Taqman, samples were isolated with  
568 trizol (Life Technologies) and further processed with the miRNeasy kit

569 (Qiagen). cDNA synthesis was performed using the TaqMan MicroRNA  
570 Reverse Transcription Kit (Life Technologies) using the corresponding oligos  
571 according to the manufacturer's recommendations.

572

573 **QPCR and PCR.**

574 PCR was performed using the KAPA2G fast mix (Kapa Biosystems) with  
575 corresponding primers. QPCR was carried out using KAPA 2G SYBRGreen  
576 (Kapa Biosystems) using the Applied Biosystems 7900HT machine with the  
577 cycling conditions: 95 °C for 3 min, 95 °C for 3 s, 60 °C for 30 s.

578 QPCR for miRNA expression analysis was performed according to the  
579 protocol for the TaqMan microRNA Assay kit (Life Technologies) with the  
580 same cycling scheme as above. Primer and probe sets for TaqMan were also  
581 purchased from Life Technologies (TaqMan® MicroRNA Assay, hsa-miR-34a,  
582 human and Control miRNA Assay, RNU48, human).

583 Primers for all PCR-based experiments are listed in **Supplementary Table 1**.

584

585 **Bi-directional promoter.**

586 The overlapping region (p1) corresponds with the sequence previously  
587 published as the TP53 binding site in (Raver-Shapira et al. 2007) which we  
588 synthesized and cloned into the pLucRluc construct (Polson et al. 2011).

589

590 **Cell-cycle distribution.**

591 Cells were washed in PBS and fixed in 4% PFA at room temperature  
592 overnight. PFA was removed, and cells were re-suspended in 95% EtOH. The  
593 samples were then rehydrated in distilled water, stained with DAPI and

594 analyzed by flow cytometry on a LSRII (BD Biosciences) machine. Resulting  
595 cell cycle phases were quantified using the ModFit software (Verity Software  
596 House).

597

598 **3'-RACE**

599 3'-RACE was performed as described as previously in (Johnsson et al. 2013).  
600 Briefly, U2OS cell RNA was polyA-tailed using yeast polyA polymerase after  
601 which cDNA was synthesized using oligo(dT) primers. Nested-PCR was  
602 performed first using a forward primer in miR34a asRNA exon 1 and a tailed  
603 oligo(dT) primer followed by a second PCR using an alternate miR34a asRNA  
604 exon 1 primer and a reverse primer binding to the tail of the previously used  
605 oligo(dT) primer. PCR products were gel purified and cloned the Strata Clone  
606 Kit (Agilent Technologies), and sequenced.

607

608 **ChIP**

609 The ChIP was performed as previously described in (Johnsson et al. 2013)  
610 with the following modifications. Cells were crosslinked in 1% formaldehyde,  
611 quenched with glycine (0.125M), and lysed in cell lysis buffer (5mM PIPES,  
612 85mM KCL, 0.5% NP40, protease inhibitor) and, sonicated in (50mM TRIS-  
613 HCL pH 8.0, 10mM EDTA, 1% SDS, protease inhibitor) using a Bioruptor  
614 Sonicator (Diagenode). Samples were incubated over night at 4°C with  
615 the *polII* antibody (Abcam: ab5095) and subsequently pulled down with  
616 Salmon Sperm DNA/Protein A Agarose (Upstate/Millipore) beads. DNA was  
617 eluted in Elution buffer (1% SDS, 100mM NaHCO3), followed by reverse  
618 crosslinking, RNaseA and protease K treatment. The DNA was eluted using

619 Qiagen PCR purification kit.

620 **Confluency Analysis**

621 **Fill this in**

622 **Pharmacological Compounds**

623 Doxorubicin was purchased from Teva (cat. nr. 021361). Actinomycin D was  
624 purchased from Sigma-Aldrich (cat. nr. A1410-2MG).

625

626 **CAGE analysis**

627 All available CAGE data from the ENCODE project (Consortium 2012) for 36  
628 cell lines was downloaded from the UCSC genome browser (Kent et al. 2002)  
629 for genome version hg19. Of these, 28 cell lines had CAGE transcription start  
630 sites (TSS) mapping to the plus strand of chromosome 1 and in regions  
631 corresponding to 200 base pairs upstream of the *lnc34a* start site (9241796 -  
632 200) and 200 base pairs upstream of the GENCODE  
633 annotated *miR34a* asRNA start site (9242263 + 200). These cell lines  
634 included: HFDPC, H1-hESC, HMEpC, HAoEC, HPIEpC, HSaVEC, GM12878,  
635 hMSC-BM, HUVEC, AG04450, hMSC-UC, IMR90, NHDF, SK-N-SH\_RA, BJ,  
636 HOB, HPC-PL, HAoAF, NHEK, HVMF, HWP, MCF-7, HepG2, hMSC-AT,  
637 NHEM.f\_M2, SkMC, NHEM\_M2, and HCH. In total 74 samples were included.  
638 17 samples were polyA-, 47 samples were polyA+, and 10 samples were total  
639 RNA. In addition, 34 samples were whole cell, 15 enriched for the cytosolic  
640 fraction, 15 enriched for the nucleolus, and 15 enriched for the nucleus. All  
641 CAGE transcription start sites were plotted and the RPKM of the individual  
642 reads was used to colour each read to indicate their relative abundance. In  
643 cases where CAGE TSS spanned identical regions, the RPMKs of the regions

644 were summed and represented as one CAGE TSS in the figure. In addition, a  
645 density plot shows the distribution of the CAGE reads in the specified  
646 interval.

647

648 **Splice junction analysis**

649 All available whole cell (i.e. non-fractionated) spliced read data originating  
650 from the Cold Spring Harbor Lab in the ENCODE project (Consortium 2012)  
651 for 38 cell lines was downloaded from the UCSC genome browser (Kent et al.  
652 2002). Of these cell lines, 36 had spliced reads mapping to the plus strand of  
653 chromosome 1 and in the region between the *lnc34a* start (9241796) and  
654 transcription termination (9257102) site (note that *miR34a* asRNA resides  
655 totally within this region). Splice junctions from the following cell lines were  
656 included in the final figure: A549, Ag04450, Bj, CD20, CD34 mobilized,  
657 Gm12878, H1hesc, Haoaf, Haoec, Hch, Helas3, Hepg2, Hfdpc, Hmec,  
658 Hmepc, Hmescat, Hmscbm, Hmscuc, Hob, Hpcpl, Hpiepc, Hsavec, Hsmm,  
659 Huvec, Hvmf, Hwp, Imr90, Mcf7, Monocd14, Nhdf, Nhek, Nhemfm2,  
660 Nhemm2, Nhlf, Skmc, and Sknsh. All splice junctions were included in the  
661 figure and coloured according to the number of reads corresponding to  
662 each. In cases where identical reads were detected multiple times, the read  
663 count was summed and represented as one read in the figure.

664

665 **Correlation analysis**

666 Erik/Jimmy should probably take this.

667

668 **Acknowledgments**

669

670 **Competing Interests**

671

672 The authors declare no competing interests.

673

674 **Figure Supplements**

675

676 List figure supplements here!

677

678 **Supplementary Figures**

679

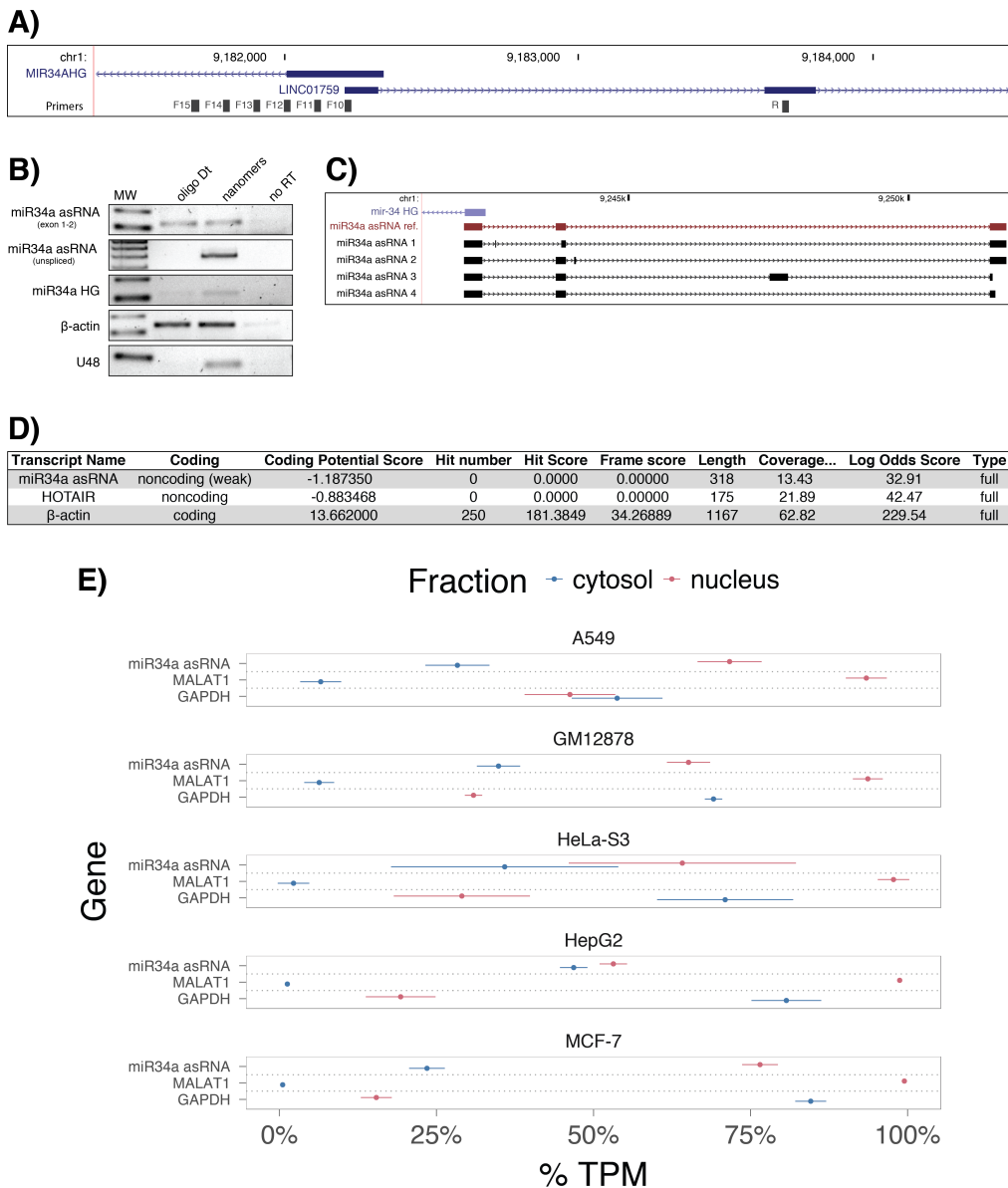
680

681  
682  
683  
684  
685  
686  
687  
688  
689

A)

cancer	n	all_R_estimate	all_pvalue	TP53wt_n	TP53wt_R_estimate	TP53wt_pvalue	TP53mut_n	TP53mut_R_estimate	TP53mut_pvalue
ACC	10	5.52e-01	1.04e-01	10	5.52e-01	1.04e-01	NA	NA	NA
BLCA	228	5.15e-01	7.89e-17	134	4.53e-01	3.86e-08	94	4.27e-01	1.73e-05
BRCA Basal	42	5.74e-01	9.54e-05	10	6.24e-01	6.02e-02	32	5.74e-01	7.41e-04
BRCA Her2	44	1.47e-01	3.39e-01	12	2.24e-01	4.85e-01	32	6.82e-02	7.10e-01
BRCA LumA	199	3.41e-01	8.22e-07	177	3.43e-01	2.96e-06	22	4.86e-01	2.31e-02
BRCA LumB	70	1.71e-01	1.57e-01	61	1.48e-01	2.53e-01	9	1.67e-01	6.78e-01
CESC	156	1.39e-01	8.37e-02	145	1.60e-01	5.45e-02	11	-4.55e-02	9.03e-01
HNSC	313	5.37e-01	8.38e-25	123	6.08e-01	0.00e+00	190	4.47e-01	9.68e-11
KICH	5	6.00e-01	3.50e-01	5	6.00e-01	3.50e-01	NA	NA	NA
KIRC	142	3.49e-01	2.06e-05	141	3.37e-01	4.41e-05	NA	NA	NA
KIRP	167	4.51e-01	9.16e-10	163	4.48e-01	2.04e-09	4	8.00e-01	3.33e-01
LGG	271	6.33e-01	9.92e-32	76	7.28e-01	0.00e+00	195	3.87e-01	2.26e-08
LIHC	153	5.63e-01	3.64e-14	114	5.16e-01	4.18e-09	39	4.55e-01	3.95e-03
LUAD	234	2.82e-01	1.15e-05	128	3.61e-01	2.87e-05	106	2.27e-01	1.91e-02
LUSC	139	2.29e-01	6.74e-03	42	4.17e-02	7.93e-01	97	3.29e-01	9.91e-04
OV	56	2.33e-01	8.37e-02	10	8.42e-01	4.46e-03	46	1.46e-01	3.31e-01
PRAD	413	4.66e-01	1.33e-23	375	4.59e-01	6.13e-21	38	4.50e-01	4.58e-03
SKCM	165	6.48e-01	5.43e-21	152	6.10e-01	7.85e-17	13	4.34e-01	1.40e-01
STAD	225	3.72e-01	8.23e-09	145	3.67e-01	5.71e-06	80	4.20e-01	1.03e-04
THCA	469	4.58e-01	1.07e-25	467	4.62e-01	4.06e-26	NA	NA	NA

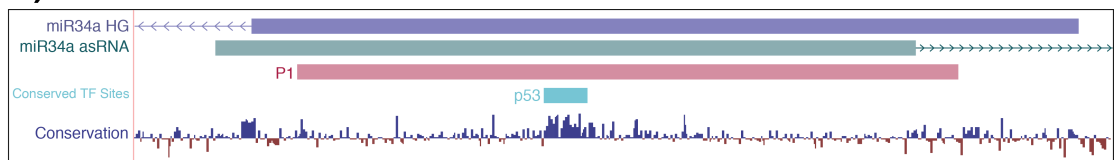
**Figure 1\_Supplement 1: A)** R-squared and p-values from the correlation analysis investigating the correlation between miR34a and miR34a asRNA expression in TP53 wild type (wt) and mutated (mut) samples within TCGA cancer types. Bladder Urothelial Carcinoma (BLCA), Breast invasive carcinoma (BRCA), Head and Neck squamous cell carcinoma (HNSC), Lower Grade Glioma (LGG), Liver hepatocellular carcinoma (LIHC), Lung adenocarcinoma (LUAD), Lung squamous cell carcinoma (LUSC), Ovarian serous cystadenocarcinoma (OV), Prostate adenocarcinoma (PRAD), Skin Cutaneous Melanoma (SKCM), Stomach adenocarcinoma (STAD).



690  
691  
692  
693  
694  
695  
696  
697  
698  
699  
700

**Figure 1 Supplement 2:** **A)** A schematic representation of the primer placement in the primer walk assay. **B)** Polyadenylation status of spliced and unspliced miR34a asRNA in HEK293T cells. **C)** Sequencing results from the analysis of *miR34a* asRNA isoforms in U2OS cells. *miR34a* AS ref. refers to the full length transcript as defined by the 3'-RACE and primer walk assay. **D)** Analysis of coding potential of the *miR34a* asRNA transcript using the Coding-potential Calculator. **E)** RNAseq data from five fractionated cell lines in the ENCODE project showing the percentage of transcripts per million (TPM) for miR34a asRNA. MALAT1 (nuclear localization) and GAPDH (cytoplasmic localization) are included as fractionation controls. Points represent the mean and horizontal lines represent the standard deviation from two biological replicates.

**A)**

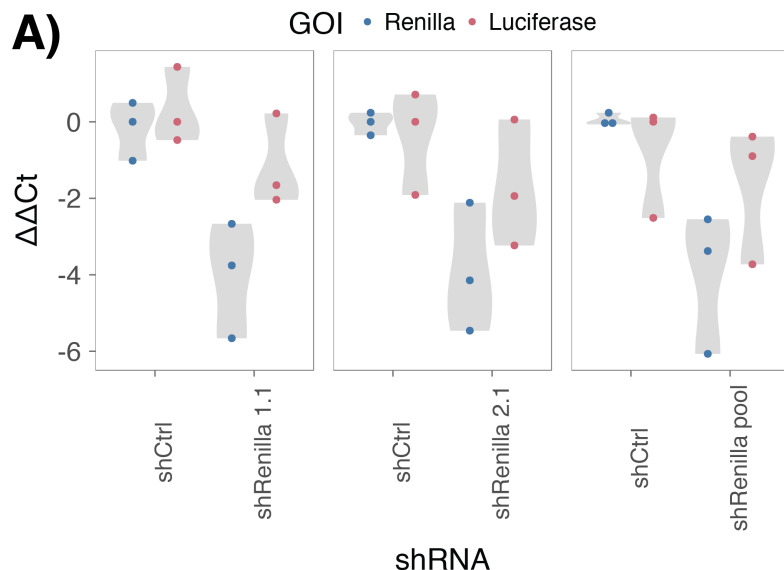


**B)**



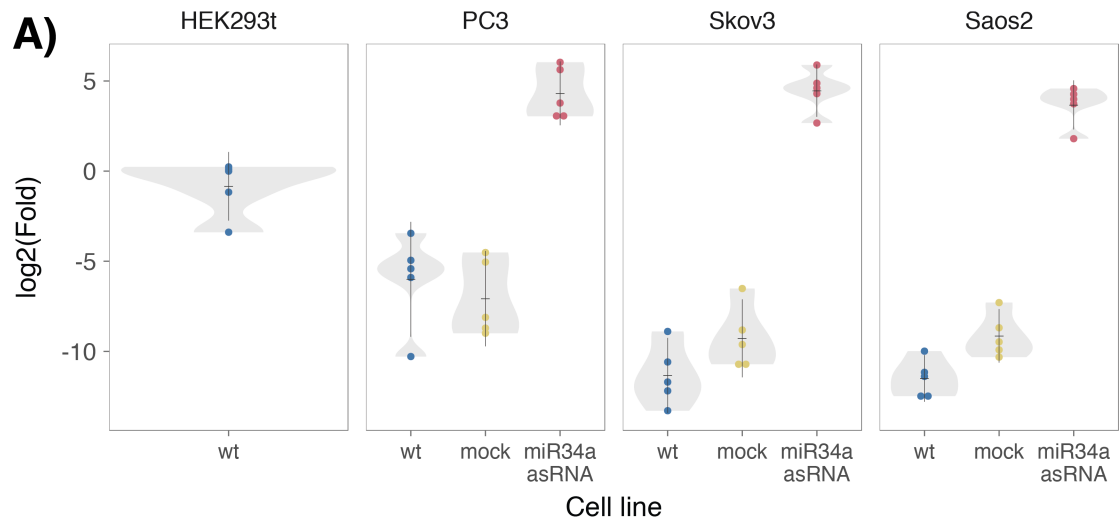
701  
702  
703  
704  
705

**Figure 2 Supplement 1:** **A)** A UCSC genome browser illustration indicating the location of the promoter region cloned into the p1 construct including the conserved TP53-binding site. **B)** A representative picture of the p1 construct including forward (F) and reverse (R) primer locations and the renilla shRNA targeting site.



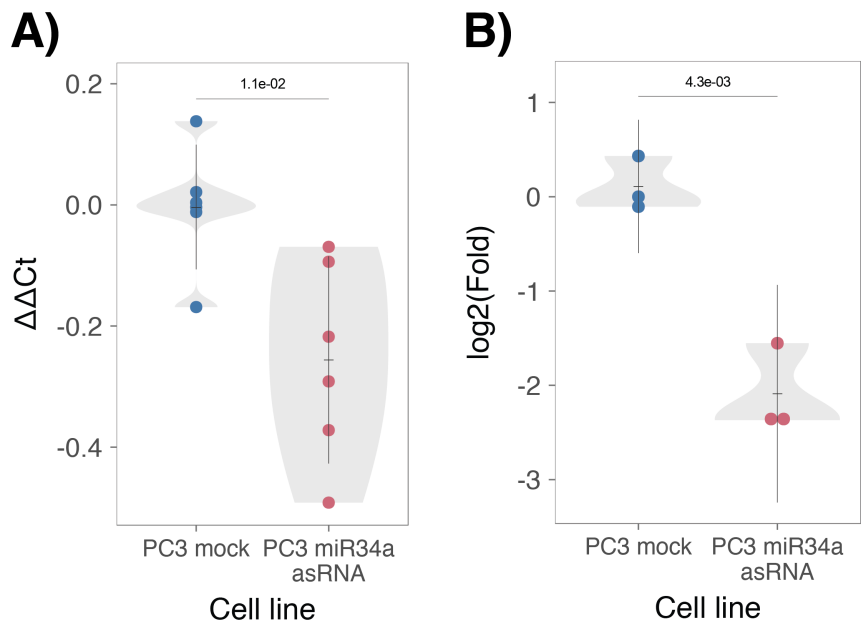
706  
707  
708  
709  
710  
711

**Figure 2 Supplement 2: A)** HEK293t cells were co-transfected with the P1 construct and either shRenilla or shControl. Renilla and luciferase levels were measured with Q-PCR 48 hours after transfection. Individual points represent independent experiments with the gray shadow indicating the density of the points.



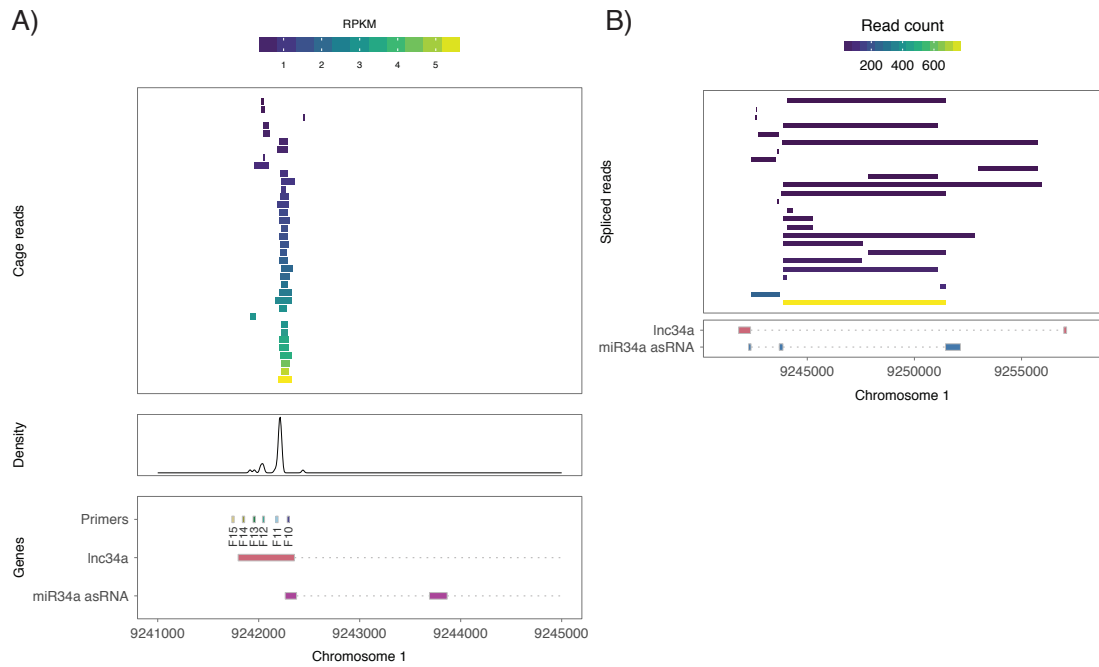
712  
713  
714  
715

**Figure 3 Supplement 1:** A) Comparison of *miR34a* asRNA expression in HEK293T cells (high endogenous *miR34a* asRNA), and the wild-type (wt), mock, and *miR34a* asRNA over-expressing stable cell lines.



716  
717  
718

**Figure 3 Supplement 2:** CCND1 expression (**A**) and protein levels (**B**) in *miR34a* over-expressing PC3 stable cell lines.



719  
720  
721  
722  
723  
724  
725  
726  
727

**Supplementary Figure 4:** A) CAGE transcription start sites from 28 ENCODE cell lines which mapped between 200 base pairs upstream of the *lnc34a* start site and 200 base pairs upstream of the GENCODE annotated *miR34a* asRNA start site (top panel). The density of the CAGE reads (middle panel) and the transcription start regions for *lnc34a* and the annotated *miR34a* asRNA, as well as, primer positions from the primer walk assay (bottom panel) are also illustrated. B) Spliced reads from 36 ENCODE cell lines which had reads mapping to the *lnc34a/miR34a* asRNA locus (top panel) and the *lnc34a* and *miR34a* asRNA genes (bottom panel).

- 728  
729 **References**  
730
- 731 Agostini, M., P. Tucci, R. Killick, E. Candi, B. S. Sayan, P. Rivetti di Val Cervo, P.  
732 Nicotera, F. McKeon, R. A. Knight, T. W. Mak and G. Melino (2011). "Neuronal  
733 differentiation by TAp73 is mediated by microRNA-34a regulation of synaptic  
734 protein targets." *Proc Natl Acad Sci U S A* **108**(52): 21093-21098. DOI:  
735 10.1073/pnas.1112061109  
736
- 737 Ahn, Y. H., D. L. Gibbons, D. Chakravarti, C. J. Creighton, Z. H. Rizvi, H. P. Adams,  
738 A. Pertsemlidis, P. A. Gregory, J. A. Wright, G. J. Goodall, E. R. Flores and J. M.  
739 Kurie (2012). "ZEB1 drives prometastatic actin cytoskeletal remodeling by  
740 downregulating miR-34a expression." *J Clin Invest* **122**(9): 3170-3183. DOI:  
741 10.1172/JCI63608  
742
- 743 Allaire, J., Y. Xie, J. McPherson, J. Luraschi, K. Ushey, A. Atkins, H. Wickham, J.  
744 Cheng and W. Chang (2017). rmarkdown: Dynamic Documents for R. R package  
745 version 1.8. <https://CRAN.R-project.org/package=rmarkdown>  
746
- 747 Amarzguioui, M., J. J. Rossi and D. Kim (2005). "Approaches for chemically  
748 synthesized siRNA and vector-mediated RNAi." *FEBS Lett* **579**(26): 5974-5981.  
749 DOI: 10.1016/j.febslet.2005.08.070  
750
- 751 Arnold, J. B. (2017). ggthemes: Extra Themes, Scales and Geoms for 'ggplot2'. R  
752 package version 3.4.0. <https://CRAN.R-project.org/package=ggthemes>  
753
- 754 Ashouri, A., V. I. Sayin, J. Van den Eynden, S. X. Singh, T. Papagiannakopoulos and  
755 E. Larsson (2016). "Pan-cancer transcriptomic analysis associates long non-coding  
756 RNAs with key mutational driver events." *Nature Communications* **7**: 13197. DOI:  
757 10.1038/ncomms13197  
758
- 759 Balbin, O. A., R. Malik, S. M. Dhanasekaran, J. R. Prensner, X. Cao, Y. M. Wu, D.  
760 Robinson, R. Wang, G. Chen, D. G. Beer, A. I. Nesvizhskii and A. M. Chinnaian  
761 (2015). "The landscape of antisense gene expression in human cancers." *Genome Res*  
762 **25**(7): 1068-1079. DOI: 10.1101/gr.180596.114  
763
- 764 Chang, T. C., D. Yu, Y. S. Lee, E. A. Wentzel, D. E. Arking, K. M. West, C. V.  
765 Dang, A. Thomas-Tikhonenko and J. T. Mendell (2008). "Widespread microRNA  
766 repression by Myc contributes to tumorigenesis." *Nat Genet* **40**(1): 43-50. DOI:  
767 10.1038/ng.2007.30  
768
- 769 Chang, W. (2014). extrafont: Tools for using fonts. R package version 0.17.  
770 <https://CRAN.R-project.org/package=extrafont>  
771
- 772 Chen, J., M. Sun, W. J. Kent, X. Huang, H. Xie, W. Wang, G. Zhou, R. Z. Shi and J.  
773 D. Rowley (2004). "Over 20% of human transcripts might form sense-antisense  
774 pairs." *Nucleic Acids Res* **32**(16): 4812-4820. DOI: 10.1093/nar/gkh818  
775
- 776 Cheng, J., L. Zhou, Q. F. Xie, H. Y. Xie, X. Y. Wei, F. Gao, C. Y. Xing, X. Xu, L. J.  
777 Li and S. S. Zheng (2010). "The impact of miR-34a on protein output in

778 hepatocellular carcinoma HepG2 cells." Proteomics **10**(8): 1557-1572. DOI:  
779 10.1002/pmic.200900646  
780  
781 Chim, C. S., K. Y. Wong, Y. Qi, F. Loong, W. L. Lam, L. G. Wong, D. Y. Jin, J. F.  
782 Costello and R. Liang (2010). "Epigenetic inactivation of the miR-34a in  
783 hematological malignancies." Carcinogenesis **31**(4): 745-750. DOI:  
784 10.1093/carcin/bgq033  
785  
786 Cole, K. A., E. F. Attiyeh, Y. P. Mosse, M. J. Laquaglia, S. J. Diskin, G. M. Brodeur  
787 and J. M. Maris (2008). "A functional screen identifies miR-34a as a candidate  
788 neuroblastoma tumor suppressor gene." Mol Cancer Res **6**(5): 735-742. DOI:  
789 10.1158/1541-7786.MCR-07-2102  
790  
791 Conley, A. B. and I. K. Jordan (2012). "Epigenetic regulation of human cis-natural  
792 antisense transcripts." Nucleic Acids Res **40**(4): 1438-1445. DOI:  
793 10.1093/nar/gkr1010  
794  
795 Consortium, E. P. (2012). "An integrated encyclopedia of DNA elements in the  
796 human genome." Nature **489**(7414): 57-74. DOI: 10.1038/nature11247  
797  
798 Core, L. J., J. J. Waterfall and J. T. Lis (2008). "Nascent RNA sequencing reveals  
799 widespread pausing and divergent initiation at human promoters." Science **322**(5909):  
800 1845-1848. DOI: 10.1126/science.1162228  
801  
802 Derrien, T., R. Johnson, G. Bussotti, A. Tanzer, S. Djebali, H. Tilgner, G. Guernec,  
803 D. Martin, A. Merkel, D. G. Knowles, J. Lagarde, L. Veeravalli, X. Ruan, Y. Ruan, T.  
804 Lassmann, P. Carninci, J. B. Brown, L. Lipovich, J. M. Gonzalez, M. Thomas, C. A.  
805 Davis, R. Shiekhattar, T. R. Gingeras, T. J. Hubbard, C. Notredame, J. Harrow and R.  
806 Guigo (2012). "The GENCODE v7 catalog of human long noncoding RNAs: analysis  
807 of their gene structure, evolution, and expression." Genome Res **22**(9): 1775-1789.  
808 DOI: 10.1101/gr.132159.111  
809  
810 Ding, N., H. Wu, T. Tao and E. Peng (2017). "NEAT1 regulates cell proliferation and  
811 apoptosis of ovarian cancer by miR-34a-5p/BCL2." Onco Targets Ther **10**: 4905-  
812 4915. DOI: 10.2147/OTT.S142446  
813  
814 Djebali, S., C. A. Davis, A. Merkel, A. Dobin, T. Lassmann, A. Mortazavi, A. Tanzer,  
815 J. Lagarde, W. Lin, F. Schlesinger, C. Xue, G. K. Marinov, J. Khatun, B. A. Williams,  
816 C. Zaleski, J. Rozowsky, M. Roder, F. Kokocinski, R. F. Abdelhamid, T. Alioto, I.  
817 Antoshechkin, M. T. Baer, N. S. Bar, P. Batut, K. Bell, I. Bell, S. Chakrabortty, X.  
818 Chen, J. Chrast, J. Curado, T. Derrien, J. Drenkow, E. Dumais, J. Dumais, R.  
819 Duttagupta, E. Falconnet, M. Fastuca, K. Fejes-Toth, P. Ferreira, S. Foissac, M. J.  
820 Fullwood, H. Gao, D. Gonzalez, A. Gordon, H. Gunawardena, C. Howald, S. Jha, R.  
821 Johnson, P. Kapranov, B. King, C. Kingswood, O. J. Luo, E. Park, K. Persaud, J. B.  
822 Preall, P. Ribeca, B. Risk, D. Robyr, M. Sammeth, L. Schaffer, L. H. See, A. Shahab,  
823 J. Skancke, A. M. Suzuki, H. Takahashi, H. Tilgner, D. Trout, N. Walters, H. Wang,  
824 J. Wrobel, Y. Yu, X. Ruan, Y. Hayashizaki, J. Harrow, M. Gerstein, T. Hubbard, A.  
825 Reymond, S. E. Antonarakis, G. Hannon, M. C. Giddings, Y. Ruan, B. Wold, P.  
826 Carninci, R. Guigo and T. R. Gingeras (2012). "Landscape of transcription in human  
827 cells." Nature **489**(7414): 101-108. DOI: 10.1038/nature11233

- 828  
829 Gallardo, E., A. Navarro, N. Vinolas, R. M. Marrades, T. Diaz, B. Gel, A. Quera, E.  
830 Bandres, J. Garcia-Foncillas, J. Ramirez and M. Monzo (2009). "miR-34a as a  
831 prognostic marker of relapse in surgically resected non-small-cell lung cancer."  
832 Carcinogenesis **30**(11): 1903-1909. DOI: 10.1093/carcin/bgp219  
833  
834 Hunten, S., M. Kaller, F. Drepper, S. Oeljeklaus, T. Bonfert, F. Erhard, A. Dueck, N.  
835 Eichner, C. C. Friedel, G. Meister, R. Zimmer, B. Warscheid and H. Hermeking  
836 (2015). "p53-Regulated Networks of Protein, mRNA, miRNA, and lncRNA  
837 Expression Revealed by Integrated Pulsed Stable Isotope Labeling With Amino Acids  
838 in Cell Culture (pSILAC) and Next Generation Sequencing (NGS) Analyses." Mol  
839 Cell Proteomics **14**(10): 2609-2629. DOI: 10.1074/mcp.M115.050237  
840  
841 International Human Genome Sequencing, C. (2004). "Finishing the euchromatic  
842 sequence of the human genome." Nature **431**(7011): 931-945. DOI:  
843 10.1038/nature03001  
844  
845 Johnsson, P., A. Ackley, L. Vidarsdottir, W. O. Lui, M. Corcoran, D. Grander and K.  
846 V. Morris (2013). "A pseudogene long-noncoding-RNA network regulates PTEN  
847 transcription and translation in human cells." Nat Struct Mol Biol **20**(4): 440-446.  
848 DOI: 10.1038/nsmb.2516  
849  
850 Katayama, S., Y. Tomaru, T. Kasukawa, K. Waki, M. Nakanishi, M. Nakamura, H.  
851 Nishida, C. C. Yap, M. Suzuki, J. Kawai, H. Suzuki, P. Carninci, Y. Hayashizaki, C.  
852 Wells, M. Frith, T. Ravasi, K. C. Pang, J. Hallinan, J. Mattick, D. A. Hume, L.  
853 Lipovich, S. Batalov, P. G. Engstrom, Y. Mizuno, M. A. Faghihi, A. Sandelin, A. M.  
854 Chalk, S. Mottagui-Tabar, Z. Liang, B. Lenhard, C. Wahlestedt, R. G. E. R. Group, G.  
855 Genome Science and F. Consortium (2005). "Antisense transcription in the  
856 mammalian transcriptome." Science **309**(5740): 1564-1566. DOI:  
857 10.1126/science.1112009  
858  
859 Kent, W. J., C. W. Sugnet, T. S. Furey, K. M. Roskin, T. H. Pringle, A. M. Zahler and  
860 D. Haussler (2002). "The human genome browser at UCSC." Genome Res **12**(6):  
861 996-1006. DOI: 10.1101/gr.229102. Article published online before print in May  
862 2002  
863  
864 Kim, K. H., H. J. Kim and T. R. Lee (2017). "Epidermal long non-coding RNAs are  
865 regulated by ultraviolet irradiation." Gene **637**: 196-202. DOI:  
866 10.1016/j.gene.2017.09.043  
867  
868 Kong, L., Y. Zhang, Z. Q. Ye, X. Q. Liu, S. Q. Zhao, L. Wei and G. Gao (2007).  
869 "CPC: assess the protein-coding potential of transcripts using sequence features and  
870 support vector machine." Nucleic Acids Res **35**(Web Server issue): W345-349. DOI:  
871 10.1093/nar/gkm391  
872  
873 Lal, A., M. P. Thomas, G. Altschuler, F. Navarro, E. O'Day, X. L. Li, C. Concepcion,  
874 Y. C. Han, J. Thiery, D. K. Rajani, A. Deutsch, O. Hofmann, A. Ventura, W. Hide  
875 and J. Lieberman (2011). "Capture of microRNA-bound mRNAs identifies the tumor  
876 suppressor miR-34a as a regulator of growth factor signaling." PLoS Genet **7**(11):  
877 e1002363. DOI: 10.1371/journal.pgen.1002363

- 878  
879 Leveille, N., C. A. Melo, K. Rooijers, A. Diaz-Lagares, S. A. Melo, G. Korkmaz, R.  
880 Lopes, F. Akbari Moqadam, A. R. Maia, P. J. Wijchers, G. Geeven, M. L. den Boer,  
881 R. Kalluri, W. de Laat, M. Esteller and R. Agami (2015). "Genome-wide profiling of  
882 p53-regulated enhancer RNAs uncovers a subset of enhancers controlled by a  
883 lncRNA." Nature Communications **6**: 6520. DOI: 10.1038/ncomms7520  
884  
885 Liu, C., K. Kelnar, B. Liu, X. Chen, T. Calhoun-Davis, H. Li, L. Patrawala, H. Yan,  
886 C. Jeter, S. Honorio, J. F. Wiggins, A. G. Bader, R. Fagin, D. Brown and D. G. Tang  
887 (2011). "The microRNA miR-34a inhibits prostate cancer stem cells and metastasis  
888 by directly repressing CD44." Nat Med **17**(2): 211-215. DOI: 10.1038/nm.2284  
889  
890 Memczak, S., M. Jens, A. Elefsinioti, F. Torti, J. Krueger, A. Rybak, L. Maier, S. D.  
891 Mackowiak, L. H. Gregersen, M. Munschauer, A. Loewer, U. Ziebold, M. Landthaler,  
892 C. Kocks, F. le Noble and N. Rajewsky (2013). "Circular RNAs are a large class of  
893 animal RNAs with regulatory potency." Nature **495**(7441): 333-338. DOI:  
894 10.1038/nature11928  
895  
896 Neil, H., C. Malabat, Y. d'Aubenton-Carafa, Z. Xu, L. M. Steinmetz and A. Jacquier  
897 (2009). "Widespread bidirectional promoters are the major source of cryptic  
898 transcripts in yeast." Nature **457**(7232): 1038-1042. DOI: 10.1038/nature07747  
899  
900 O'Leary, N. A., M. W. Wright, J. R. Brister, S. Ciufo, D. Haddad, R. McVeigh, B.  
901 Rajput, B. Robbertse, B. Smith-White, D. Ako-Adjei, A. Astashyn, A. Badretdin, Y.  
902 Bao, O. Blinkova, V. Brover, V. Chetvernin, J. Choi, E. Cox, O. Ermolaeva, C. M.  
903 Farrell, T. Goldfarb, T. Gupta, D. Haft, E. Hatcher, W. Hlavina, V. S. Joardar, V. K.  
904 Kodali, W. Li, D. Maglott, P. Masterson, K. M. McGarvey, M. R. Murphy, K.  
905 O'Neill, S. Pujar, S. H. Rangwala, D. Rausch, L. D. Riddick, C. Schoch, A. Shkeda,  
906 S. S. Storz, H. Sun, F. Thibaud-Nissen, I. Tolstoy, R. E. Tully, A. R. Vatsan, C.  
907 Wallin, D. Webb, W. Wu, M. J. Landrum, A. Kimchi, T. Tatusova, M. DiCuccio, P.  
908 Kitts, T. D. Murphy and K. D. Pruitt (2016). "Reference sequence (RefSeq) database  
909 at NCBI: current status, taxonomic expansion, and functional annotation." Nucleic  
910 Acids Res **44**(D1): D733-745. DOI: 10.1093/nar/gkv1189  
911  
912 Ozsolak, F., P. Kapranov, S. Foissac, S. W. Kim, E. Fishilevich, A. P. Monaghan, B.  
913 John and P. M. Milos (2010). "Comprehensive polyadenylation site maps in yeast and  
914 human reveal pervasive alternative polyadenylation." Cell **143**(6): 1018-1029. DOI:  
915 10.1016/j.cell.2010.11.020  
916  
917 Pelechano, V. and L. M. Steinmetz (2013). "Gene regulation by antisense  
918 transcription." Nat Rev Genet **14**(12): 880-893. DOI: 10.1038/nrg3594  
919  
920 Polson, A., E. Durrett and D. Reisman (2011). "A bidirectional promoter reporter  
921 vector for the analysis of the p53/WDR79 dual regulatory element." Plasmid **66**(3):  
922 169-179. DOI: 10.1016/j.plasmid.2011.08.004  
923  
924 Rashi-Elkeles, S., H. J. Warnatz, R. Elkon, A. Kupershtain, Y. Chobod, A. Paz, V.  
925 Amstislavskiy, M. Sultan, H. Safer, W. Nietfeld, H. Lehrach, R. Shamir, M. L. Yaspo  
926 and Y. Shiloh (2014). "Parallel profiling of the transcriptome, cistrome, and

- 927 epigenome in the cellular response to ionizing radiation." Sci Signal **7**(325): rs3. DOI:  
928 10.1126/scisignal.2005032
- 929
- 930 Raver-Shapira, N., E. Marciano, E. Meiri, Y. Spector, N. Rosenfeld, N. Moskovits, Z.  
931 Bentwich and M. Oren (2007). "Transcriptional activation of miR-34a contributes to  
932 p53-mediated apoptosis." Mol Cell **26**(5): 731-743. DOI:  
933 10.1016/j.molcel.2007.05.017
- 934
- 935 Rinn, J. L., M. Kertesz, J. K. Wang, S. L. Squazzo, X. Xu, S. A. Brugmann, L. H.  
936 Goodnough, J. A. Helms, P. J. Farnham, E. Segal and H. Y. Chang (2007).  
937 "Functional demarcation of active and silent chromatin domains in human HOX loci  
938 by noncoding RNAs." Cell **129**(7): 1311-1323. DOI: 10.1016/j.cell.2007.05.022
- 939
- 940 Rokavec, M., M. G. Oner, H. Li, R. Jackstadt, L. Jiang, D. Lodygin, M. Kaller, D.  
941 Horst, P. K. Ziegler, S. Schwitalla, J. Slotta-Huspenina, F. G. Bader, F. R. Greten and  
942 H. Hermeking (2015). "Corrigendum. IL-6R/STAT3/miR-34a feedback loop  
943 promotes EMT-mediated colorectal cancer invasion and metastasis." J Clin Invest  
944 **125**(3): 1362. DOI: 10.1172/JCI81340
- 945
- 946 Schneider, C. A., W. S. Rasband and K. W. Eliceiri (2012). "NIH Image to ImageJ:  
947 25 years of image analysis." Nat Methods **9**(7): 671-675.
- 948
- 949 Seila, A. C., J. M. Calabrese, S. S. Levine, G. W. Yeo, P. B. Rahl, R. A. Flynn, R. A.  
950 Young and P. A. Sharp (2008). "Divergent transcription from active promoters."  
951 Science **322**(5909): 1849-1851. DOI: 10.1126/science.1162253
- 952
- 953 Serviss, J. T. (2017). miR34AasRNAProject.  
954 [https://github.com/GranderLab/miR34a\\_asRNA\\_project](https://github.com/GranderLab/miR34a_asRNA_project)
- 955
- 956 Sigova, A. A., A. C. Mullen, B. Molinie, S. Gupta, D. A. Orlando, M. G. Guenther,  
957 A. E. Almada, C. Lin, P. A. Sharp, C. C. Giallourakis and R. A. Young (2013).  
958 "Divergent transcription of long noncoding RNA/mRNA gene pairs in embryonic  
959 stem cells." Proc Natl Acad Sci U S A **110**(8): 2876-2881. DOI:  
960 10.1073/pnas.1221904110
- 961
- 962 Slabakova, E., Z. Culig, J. Remsik and K. Soucek (2017). "Alternative mechanisms of  
963 miR-34a regulation in cancer." Cell Death Dis **8**(10): e3100. DOI:  
964 10.1038/cddis.2017.495
- 965
- 966 Spizzo, R., M. I. Almeida, A. Colombatti and G. A. Calin (2012). "Long non-coding  
967 RNAs and cancer: a new frontier of translational research?" Oncogene **31**(43): 4577-  
968 4587. DOI: 10.1038/onc.2011.621
- 969
- 970 Stahlhut, C. and F. J. Slack (2015). "Combinatorial Action of MicroRNAs let-7 and  
971 miR-34 Effectively Synergizes with Erlotinib to Suppress Non-small Cell Lung  
972 Cancer Cell Proliferation." Cell Cycle **14**(13): 2171-2180. DOI:  
973 10.1080/15384101.2014.1003008
- 974
- 975 Struhl, K. (2007). "Transcriptional noise and the fidelity of initiation by RNA  
976 polymerase II." Nat Struct Mol Biol **14**(2): 103-105. DOI: 10.1038/nsmb0207-103

- 977  
978 Su, X., D. Chakravarti, M. S. Cho, L. Liu, Y. J. Gi, Y. L. Lin, M. L. Leung, A. El-  
979 Naggar, C. J. Creighton, M. B. Suraokar, I. Wistuba and E. R. Flores (2010). "TAp63  
980 suppresses metastasis through coordinate regulation of Dicer and miRNAs." *Nature*  
981 **467**(7318): 986-990. DOI: 10.1038/nature09459
- 982  
983 Sun, F., H. Fu, Q. Liu, Y. Tie, J. Zhu, R. Xing, Z. Sun and X. Zheng (2008).  
984 "Downregulation of CCND1 and CDK6 by miR-34a induces cell cycle arrest." *FEBS*  
985 *Lett* **582**(10): 1564-1568. DOI: 10.1016/j.febslet.2008.03.057
- 986  
987 Team, R. C. (2017). "R: A Language and Environment for Statistical Computing."  
988 from <https://www.R-project.org/>.
- 989  
990 Turner, A. M., A. M. Ackley, M. A. Matrone and K. V. Morris (2012).  
991 "Characterization of an HIV-targeted transcriptional gene-silencing RNA in primary  
992 cells." *Hum Gene Ther* **23**(5): 473-483. DOI: 10.1089/hum.2011.165
- 993  
994 Vanhee-Brossollet, C. and C. Vaquero (1998). "Do natural antisense transcripts make  
995 sense in eukaryotes?" *Gene* **211**(1): 1-9.
- 996  
997 Vogt, M., J. Mundig, M. Gruner, S. T. Liffers, B. Verdoodt, J. Hauk, L.  
998 Steinstraesser, A. Tannapfel and H. Hermeking (2011). "Frequent concomitant  
999 inactivation of miR-34a and miR-34b/c by CpG methylation in colorectal, pancreatic,  
1000 mammary, ovarian, urothelial, and renal cell carcinomas and soft tissue sarcomas."  
1001 *Virchows Arch* **458**(3): 313-322. DOI: 10.1007/s00428-010-1030-5
- 1002  
1003 Wagner, E. G. and R. W. Simons (1994). "Antisense RNA control in bacteria, phages,  
1004 and plasmids." *Annu Rev Microbiol* **48**: 713-742. DOI:  
1005 10.1146/annurev.mi.48.100194.003433
- 1006  
1007 Wang, L., P. Bu, Y. Ai, T. Srinivasan, H. J. Chen, K. Xiang, S. M. Lipkin and X.  
1008 Shen (2016). "A long non-coding RNA targets microRNA miR-34a to regulate colon  
1009 cancer stem cell asymmetric division." *eLife* **5**. DOI: 10.7554/eLife.14620
- 1010  
1011 Wang, L., H. J. Park, S. Dasari, S. Wang, J. P. Kocher and W. Li (2013). "CPAT:  
1012 Coding-Potential Assessment Tool using an alignment-free logistic regression  
1013 model." *Nucleic Acids Res* **41**(6): e74. DOI: 10.1093/nar/gkt006
- 1014  
1015 Wang, X., J. Li, K. Dong, F. Lin, M. Long, Y. Ouyang, J. Wei, X. Chen, Y. Weng, T.  
1016 He and H. Zhang (2015). "Tumor suppressor miR-34a targets PD-L1 and functions as  
1017 a potential immunotherapeutic target in acute myeloid leukemia." *Cell Signal* **27**(3):  
1018 443-452. DOI: 10.1016/j.cellsig.2014.12.003
- 1019  
1020 Wickham, H. (2016). gtable: Arrange 'Grobs' in Tables. R package version 0.2.0.  
1021 <https://CRAN.R-project.org/package=gtable>
- 1022  
1023 Wickham, H. (2017). scales: Scale Functions for Visualization. R package version  
1024 0.5.0. <https://CRAN.R-project.org/package=scales>
- 1025

- 1026 Wickham, H. (2017). tidyverse: Easily Install and Load the 'Tidyverse'. R package  
1027 version 1.2.1. <https://CRAN.R-project.org/package=tidyverse>
- 1028
- 1029 Wickham, L. H. a. H. (2017). rlang: Functions for Base Types and Core R and  
1030 'Tidyverse' Features. R package version 0.1.4. <https://CRAN.R->  
1031 [project.org/package=rlang](https://CRAN.R-project.org/package=rlang)
- 1032
- 1033 Wickham, S. M. B. a. H. (2014). magrittr: A Forward-Pipe Operator for R. R package  
1034 version 1.5. <https://CRAN.R-project.org/package=magrittr>
- 1035
- 1036 Wilkins, D. gggenes: Draw Gene Arrow Maps in 'ggplot2'. R package version  
1037 0.2.0.9003. <https://github.com/wilcox/gggenes>
- 1038
- 1039 Xiao, N. (2017). liftr: Containerize R Markdown Documents. R package version 0.7.  
1040 <https://CRAN.R-project.org/package=liftr>
- 1041
- 1042 Xie, Y. (2017). knitr: A General-Purpose Package for Dynamic Report Generation in  
1043 R. R package version 1.17. <https://yihui.name/knitr/>
- 1044
- 1045 Yang, P., Q. J. Li, Y. Feng, Y. Zhang, G. J. Markowitz, S. Ning, Y. Deng, J. Zhao, S.  
1046 Jiang, Y. Yuan, H. Y. Wang, S. Q. Cheng, D. Xie and X. F. Wang (2012). "TGF-beta-  
1047 miR-34a-CCL22 signaling-induced Treg cell recruitment promotes venous metastases  
1048 of HBV-positive hepatocellular carcinoma." *Cancer Cell* **22**(3): 291-303. DOI:  
1049 10.1016/j.ccr.2012.07.023
- 1050
- 1051 Yap, K. L., S. Li, A. M. Munoz-Cabello, S. Raguz, L. Zeng, S. Mujtaba, J. Gil, M. J.  
1052 Walsh and M. M. Zhou (2010). "Molecular interplay of the noncoding RNA ANRIL  
1053 and methylated histone H3 lysine 27 by polycomb CBX7 in transcriptional silencing  
1054 of INK4a." *Mol Cell* **38**(5): 662-674. DOI: 10.1016/j.molcel.2010.03.021
- 1055
- 1056 Zenz, T., J. Mohr, E. Eldering, A. P. Kater, A. Buhler, D. Kienle, D. Winkler, J.  
1057 Durig, M. H. van Oers, D. Mertens, H. Dohner and S. Stilgenbauer (2009). "miR-34a  
1058 as part of the resistance network in chronic lymphocytic leukemia." *Blood* **113**(16):  
1059 3801-3808. DOI: 10.1182/blood-2008-08-172254
- 1060
- 1061